

**SEISMIC INTERPRETATION, PETROPHYSICS AND  
COLORED INVERSION OF FIMKASSAR AREA, UPPER  
INDUS BASIN, PAKISTAN**



**BY**

**MUHAMMAD AZAM KHAN**

**BS-GEOPHYSICS**

**(2014-2018)**

**DEPARTMENT OF EARTH SCIENCES**

**QUAID-I-AZAM UNIVERSITY**

**ISLAMABAD**

## **CERTIFICATE OF APPROVAL**

This dissertation submitted by **MUHAMMAD AZAM KHAN** is accepted in its present form by the Department of Earth Sciences, Quaid-i-Azam University Islamabad as satisfying the requirement for the award of degree of BS-Geophysics.

### **RECOMMENDED BY**

**PROF. DR. MONA LISA**

(Supervisor)

\_\_\_\_\_

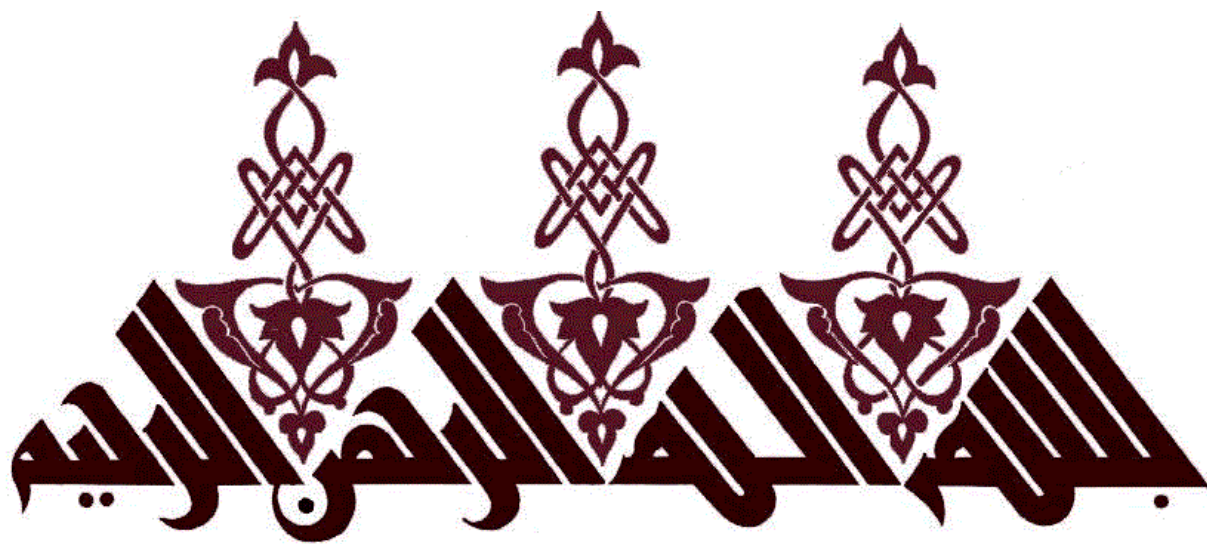
**PROF. DR. MONA LISA**

(Chairperson Department of earth sciences)

\_\_\_\_\_

**EXTERNAL EXAMINER**

\_\_\_\_\_



# DEDICATION

*I would like to dedicate this thesis work to my sweet parents, whose love, encouragement, guidance and prayers make me able to achieve such success and honor.*

## **ACKNOWLEDGEMENT**

First praise is to Allah, the most Beneficent, Merciful and Almighty, on whom ultimately we depend for sustenance and guidance. I bear witness that Holy Prophet Muhammad (PBUH) is the last messenger, whose life is perfect model for the whole mankind till the Day of Judgment. I thank Allah for giving me strength and ability to complete this study.

I am especially indebted to my honorable supervisor **PROF. DR. MONA LISA** for giving me an initiative to this study. I express my sincerest appreciation to **Mr. ZAHID ULLAH** and **Mr. Mukhtar** for their guidance in the preparation of this thesis and assistance in any way that I may have asked.

I specially acknowledge the prayers and efforts of my whole family, specially my parents for their encouragement, support and sacrifices throughout the study. I also wish to thank the whole faculty of my department for providing me with an academic base, which has enabled me to take up this study I pay my thanks to the employees of clerical office who helped me a lot and all those their names do not appear here who have contributed to the successful completion of this study.

## **ABSTRACT**

The dissertation work includes seismic data interpretation, Petro physical analysis using well logs data; identification of possible resource plays as well use of seismic inversion to estimate physical properties of rocks.

Seismic and well log interpretation used for study of structural style, physical properties of rocks and identification of possible petroleum system of Fimkassar area (Upper Indus Basin) Pakistan.

Well locations are proposed by constructing time and a depth contour map which shows faulted anticline in study area, two leads are shown on these contours. These two leads are marked on Chorgali, Sakesar and Patala Formations. Petrophysical analysis of wells TURKWAL-01 is carried out for Chorgali, Sakesar and Patala Formations in order to depict the probable hydrocarbon producing reservoir. The results suggest that both Chorgali and Sakesar Formations are more producing as compared to Nammal Formation which is less productive because of alternating shale limestone lithologies. Patala Formation is found to be mature source rock with in some wells of study area, while Nammal Formation consists of immature organic content. The lower part of Sakesar Formation shows indication of maturity or reservoir shale.

Seismic inversion results are also demonstrating that Chorgali act as a reservoir. The post stack color inversion is performed to confirm the leads location. On inverted section Chorgali shows low value of impedance i.e. strong indicator for the presence of hydrocarbons.

## Contents

<b>INTRODUCTION.....</b>	<b>1</b>
1.1 Introduction .....	2
1.2 Exploration History Of Fimkassar Oil Field .....	3
1.3 Objectivef Dissertation .....	3
1.4 Data Used .....	4
1.5 Software Tools Used .....	4
1.6 Geographical Location .....	5
1.7 Methodology.....	6
<b>GEOLOGY.....</b>	<b>7</b>
2.1 Regional Tectonic Setting .....	8
2.2 Geological Boundary .....	8
2.2.1 Kalabagh Fault.....	8
2.2.2 Jhelum Fault .....	9
2.2.3 Salt Range Thrust .....	9
2.2.4 Main Boundary Thrust.....	9
2.3 Tectonics Of Eastern Potwar Basin .....	10
2.4 Stratigraphy Of The Area .....	11
2.5 Petroleum Prospect .....	12
2.5.1 Source Rocks .....	12
2.5.2 Resorvoir Rocks .....	13
2.5.3 Trap Or Seal Rocks.....	13
<b>INTERPRETATION OF SEISMIC DATA.....</b>	<b>17</b>
3.1 Seismic Interpretation.....	17
3.2 Base Map .....	17
3.3 Interpretation Of Seismic Lines.....	17
3.4 Interpreted Of Seismic Section.....	17
3.5 Fault Polygons Generation .....	19
3.6 Contour Maps .....	20
3.7 Time And Depth Contour Maps Of Chorgali Formation .....	21

3.8	Time And Depth Contour Map Of Sakeser Formation .....	23
3.9	Time And Depth Contour Of Patala Formation .....	24
3.10	Identification Of Well Location .....	26
3.10.1	Lead-01.....	26
3.10.2	Lead-02.....	26
3.11	Seismic Attributes.....	28
3.11.1	Average Energy.....	28
3.11.2	Instantaneous Phase.....	28
3.11.2	Trace Envelope.....	28
<b>PETROPHYSICS .....</b>		<b>30</b>
4.1	Introduction .....	31
4.2	Petrophysical Analysis .....	31
4.3	Estimation Of Volume Of Shale .....	31
4.4	Estimation Of Porosity.....	32
4.4.1	Calculation Of Porosity From Sonic Log.....	32
4.4.2	Calculation Of Porosity From Density Log .....	33
4.4.3	Calculation Of Porosity From Neutron Log.....	33
4.5	Total Porosity .....	34
4.6	Estimation Of Water Saturation .....	34
4.6.1	Estimation Of True Resistivity.....	35
4.6.2	Estimation Of Resistivity Of Water ( ).....	36
4.7	Estimation Of Hydrocarbon Saturation .....	38
4.8	Estimation Of Permeability .....	38
4.9	Well Log Interpretation Of Turkwal-01 .....	39
4.10	Cross- Plot Of Neutron And Density Log .....	40
<b>COLORED INVERSION OF POST STACK DATA.....</b>		<b>42</b>
5.1	Wavelet and acoustic impedance .....	43
5.2	Methodology.....	45
5.3	Non uniqueness and convolution .....	45



5.4	Wavelet extraction.....	46
5.5	Impedance estimation.....	46
5.6	Butterworth filter.....	47
5.7	Interpretation of inverted section.....	51
5.8	Confirmation of lead-02 .....	51
	Conclusion .....	53
	References.....	54

## **List of figures:**

- Figure (1.1): A schematic diagram describing forward and inverse problem.
- Figure (1.2): Satellite image of Fimkassar area.
- Figure (2.1): Tectonic map (Banks and Warburton
- Figure (2.2): Stratigraphic chart of the area. (Aamir and Siddiqui, 2006).
- Figure (3.1): Flow chart of Interpretation.
- Figure (3.2): Base map of the Fimkassar area.
- Figure (3.3): Interpreted seismic line PW-04.
- Figure (3.4): Interpreted seismic line PW-02
- Figure (3.5): Polygon's orientation on base map.
- Figure (3.6): TWT contour map of Chorgali Formation.
- Figure (3.7): Depth contour map of Chorgali Formation.
- Figure (3.8): TWT contour map of Sakesar Formation.
- Figure (3.9): Depth contour map of Sakesar Formation.
- Figure (3.10): TWT contour map of Patala Formation.
- Figure (3.11): Depth contour map of Patala Formation.
- Figure (3.12): Identification of leads of Chorgali Formation.
- Figure (3.13): Identification of Leads of Sakesar Formation.
- Figure (3.14): Identification of Leads of Patala Formation
- Figure (3.15): Average energy attribute calculated for seismic line 96 -PW-04.
- Figure (3.16): Instantaneous phase attribute calculated for seismic line 96-PW-01.
- Figure (3.17): Identification of signal envelope for seismic line 96-PW-01
- Figure (4.1): Determination of  $R_{weq}$  from SP chart (Schlumberger, 1989).
- Figure (4.2): Determination of  $R_w$  from SP chart (Schlumberger, 1989)
- Figure (4.3): Petrophysical analysis of Chorgali Formation in well Turkwal-01
- Figure (4.4): Cross plot of RHOB vs. NPHI using GR as color code for Chorgali Formation in Turkwal-01
- Figure (5.1): A flow chart showing impedance and wavelet extraction scheme.
- Figure (5.2): Extracted Wavelet

- Figure (5.3): Impedance spectrum with fitted line
- Figure (5.4): Butterworth filter.
- Figure (5.5): Desired and modeled spectrum.
- Figure (5.6): Shaping spectrum.
- Figure (5.7): Convolution of shaped seismic spectrum and desired spectrum.
- Figure (5.8): Convolution of seismic mean spectrum and desired spectrum.
- Figure (5.9): Input seismic section and inverted section along with logs.
- Figure (5.10): Inverted section with inverted logs
- Figure (5.11): Inverted seismic section
- Figure (5.12): Zoomed view of inverted section.
- Figure (5.13): Highlights snaked head structure at inverted section.
- Figure (5.14): Zoomed view of snaked head structure i.e. lead-02.

# **C**hapter#01

# **INTRODUCTION**

## 1.1 INTRODUCTION:

Seismic exploration method is used in hydrocarbon exploration; no doubt hydrocarbon exploration is a backbone for economy of any country, especially developing countries like Pakistan. As the energy demand increases, exploration sector catch their eyes over unexplored areas for new energy resources excavation. The dissertation comprises of exploration result in Fimkassar oil field which lies in Chakwal city Punjab province.

Geophysicists have been trying for hydrocarbon exploration since a long time ago and developed many techniques in this regard. Seismic method is direct result evaluating and accurate geophysical method used for structural analysis. Seismic Reflection Method most commonly used in hydrocarbon exploration in petroleum geology. Petroleum system mainly comprises of three constituents that are enlisted below.

- Source rocks (contains organic materials which for responsible for generation of hydrocarbons).
- Reservoir rocks (migration of hydrocarbons takes place from source rock and reservoir rock offers suitable conditions for their accumulation).
- Seal or trap rocks (act as a barrier it stops upward movement of hydrocarbons).

Investigation of earth through geophysical method involves taking measurement in order to check the variation in the physical properties of the earth both laterally and horizontally to interpret structure you can say petroleum play more precisely. (Bust et al., 2010).

Petrophysics is one of the most important and reliable technique in the field of the earth sciences. Petrophysics provide the link between the rock properties i.e. lithology, water saturation, porosity, clay content, acoustic impedance, primary and secondary wave velocity, and elastic moduli. After obtaining petrophysics results we get more clear understanding of rock properties and detect more meaningful results.

The scheme of seismic inversion is illustrated in figure (1.1) below. Generally, forward modeling is the way to go for estimation of required physical properties. However, in inversion a description of earth model parameters from recorded observations. For many interpretation applications it becomes necessary to perform inversion because it describes physical properties of whole reservoir rock that is not possible from well log data.

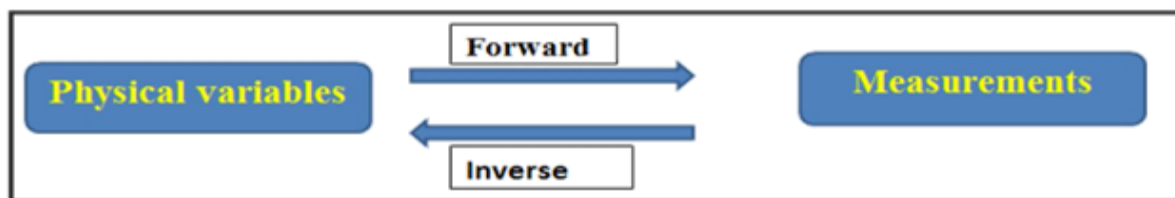


**Figure (1.1): A schematic diagram describing forward and inverse problem.**

## **1.2 EXPLORATION HISTORY OF FIMKASSAR OIL FIELD:**

Fimkassar oil and gas field is located about 75 kilometers Southwest (SW) of Islamabad, in the northern Pakistan. The field was discovered in 1980 by Gulf Oil Company (GOC), which drilled a well named, the Fimkassar-1X. The Fimkassar field produces, from Eocene limestone of Sakesar and Chorgali Formations. These Formations are deformed in an anticlinal structure known as the Fimkassar Structure. Because of low production, 20 barrels of oil per day, the field was declared non-commercial field and was sold to a local company of Pakistan, Oil and Gas Development Corporation Limited (OGDCL).

OGDCL drilled a well named, Fimkassar-1A but the well was abandoned due to technical problems. The Fimkassar-1X borehole was re-entered and sidetracked; this well was renamed as Fimkassar-1-ST. Fimkassar-1-ST was the highest oil volume producer well and it produced about 4,000 barrels/day. In 1990, well named as Fimkassar-2 was drilled. This well initially produced 1960 barrels of oil per day. Due to decrease in Formation pressure and consequently decrease in production, an injection well named as Fimkassar-3 was drilled. In 2004, a well named as Fimkassar-4 was drilled but it produced very low quantity of oil, therefore the well was plugged and abandoned.

Fimkassar is an unusual play as it produces oil and gas from a very stiff limestone that have very low porosity and permeability. Epigenetic process of dolomitization creates porosity values of 25% (Malik *et al.*, 1988), whereas tectonic deformation of the Fimkassar structure has created fractures through which hydrocarbons can migrate. Mianwali (Triassic), Datta (Jurassic), and Patala (Paleocene) Formations are major source of oil at Fimkassar field (Khan *et al.*, 1986). The Shales of Murree Formation provide a seal for hydrocarbon catch for underlying reservoirs of Eocene age.

## **1.3 OBJECTIVES OF DISSERTATION:**

The main objective of dissertation is to present a subsurface model, estimates the reservoir properties and to identify the new well location. All objectives are stated below in points.

- Detailed seismic interpretation for identification of the structures favorable for hydrocarbon accumulation.
- Petrophysical analysis for the identification of the reservoir types and various petrophysical properties of reservoir encountered in study area.
- Colored Inversion of post stack data is carried out to confirm possible lead location after estimating the various reservoir properties.

#### 1.4 DATA USED:

To achieve all the objectives, seismic and borehole data given in Table-1.1 and 1.2 is used provided by DGPC for completion this dissertation.

Seismic Lines	Direction	Seismic Lines	Direction
POL/96-PW-01	Dip Line	0884-FMK-107	Dip Line
POL/96-PW-02	Dip Line	0884-FMK-108	Dip Line
POL/96-PW-03	Dip Line	0884-FMK-106	Strike
POL/96-PW-04	Dip Line		

Table-1.1

Turkwal-01	3245	3067	Development	Oil & Gas
------------	------	------	-------------	-----------

Table-1.2

#### 1.5 SOFTWARE TOOLS USED:

To complete project and completion of this dissertation course work I used following software tools

- SMT KINGDOM 8.8
- Matlab Inc. 2010
- SnagIt 11 (Editor)

## 1.6 GEOGRAPHICAL LOCATION:

The Fimkassar field is located in the eastern part of the Potwar basin and is approximately 75 kilometers SW of Islamabad. Geographically, Fimkassar field is located in Chakwal district of Punjab province. Geologically it is located in eastern part of Potwar Basin, Upper Indus basin, bounded by Soan syncline in the north, Salt Ranges in the south, Jhelum fault in east and Kalabagh fault in west (Siddiqui *et al.*, 1998).



Figure (1.2): Satellite image of Fimkassar area.

## 1.7 SEQUENCE OF DISSERTATION:

This dissertation is divided into five chapters with first chapter forming an introduction. The 2nd chapter covers geological setting and tectonic history of the study area. The third Chapter covers the important aspect of this dissertation i.e. Interpretation of seismic data. The fourth chapter deals with Petro-physical analysis of reservoir rock using well-log data. Fifth chapter covers the colored inversion of post stack data to confirm lead location after calculating reservoir properties. The following methodologies were adopted to complete this dissertation.



## 1.8 METHODOLOGY:

- Collection of geological & Geophysical data.
- Preparation of base map.
- Marking of faults on seismic sections.
- Marking of interested reflectors on seismic sections.
- Determination of horizons by generating 1-D synthetic seismogram.
- Finding velocity of horizon using well data.
- TWT contour map generation.
- Depth contouring.
- Petrophysical properties of reservoir rock with the help of log data.
- Colored inversions of post stack data.
- Conclusions.

# Chapter#02

# GEOLOGY

## **2.1 REGIONAL TECTONIC SETTING:**

The building of Himalayan mountain process in Eocene triggered compressional system. Northward movement of Indian plate is about 40mm/year (1.6 inches/year) and is colliding with Eurasian plate. 55 million years ago Indian plate collided with the Eurasian plate and building of Himalayan mountain belt 30-40 million years was formed in the North Western Pakistan and mountain ranges moved in the east west direction (Kazmi and Jan, 1997). Being one of the most active collision zones in the world foreland thrusting is taking place on continental scale. It has created variety of active folds and thrust wedges with in Pakistan passing from Kashmir fold and thrust belt in North East, South West through the Salt Range-Potwar plateau fold belt, the Suleiman fold belt and the Makran accretionary wedge of Pakistan. As far as the Indian plate is concerned which is subducting under the Eurasian plate at its Northern edge, a sequence of north dipping south thrusts are being produced. The shortening of crust caused a large amount of folds and thrust belt. The youngest basins in the Western Himalayan Foreland Thrust Belt are Kohat Plateau, Bannu Basin and Potwar Plateau which have compressive stresses and convergent tectonics. Pakistan isolated at in the two domains Gondwanian and the Tethyan Domains (Kazmi& Jan, 1997). The south eastern part of Pakistan belongs to Gondwanian Domain and is supported by the Indo-Pakistan crustal plate whereas then or then-most and western areas of Pakistan fall in Tethyan.

## **2.2 GEOLOGICAL BOUNDARY:**

The Potwar is bounded by the following two strike-slips and two thrust faults which are.

- Kalabagh Fault.
- Jhelum Fault.
- Salt Range Thrust.
- Main Boundary Thrust.

### **2.2.1 KALABAGH FAULT:**

It is right lateral strike-slip fault and its direction is from north to west 150 km which can be seen as faulted block. It lies in the north of the Kalabagh City, Mianwali and is the Trans-Indus extension of Western Salt Range (McDougal & Khan, 1990).

### **2.2.2 JHELUM FAULT:**

Extending from Kohala to Azad Pattan the Murree is hanging while Kamlial, Chingi and Nagri Formations are footwall. Starting from the Indus-Kohistan to Ravi it is the active aspect of the Indian Shield. It is seen also in the map that MBT, Panjal Thrust and HFT cut shortened by left-lateral reverse Jhelum Fault in west (Baig, Lawrence, 1987).

### **2.2.3 SALT RANGE THRUST:**

It is also known as Himalayan Frontal Thrust. Salt range and Trans-Indus Himalayan ranges are the foothills.

### **2.2.4 MAIN BOUNDARY THRUST:**

The MBT which lies in the north of the Islamabad is called as Murree fault. The western part of this fault is orienting to north east forming non-striking fault in its western part i.e. Hazara Kashmir-Syntaxes (Latif, 1970; Yeats and Lawrence, 1984; Greco, 1991) also this fault strike the direction of east moving in the direction of Southern side of Kalachitta Range and North of Kohat plateau (Meissner et al, 1974). In Potwar the structure trend is east to west or northeast to south west end mostly large surface anticlines are bounded by the thrust or reverse faults. The structure of Potwar basin is affected by compressional forces, basement slope, and variable thickness of Pre-Cambrian salt over the basement, and deposition of very thick molasses and tectonic events. In Potwar basin some surface features mismatch subsurface structures due to décollements at different levels. In such circumstances, it is necessary to integrate seismic data with surface geological information for precise delineation of sub-surface configuration of various structures (Moghal et al, 2007). Tectonic of the potwar plateau is controlled mainly by the following factors:

1. Slope of the basement (steeper in western Potwar Plateau).
2. Thickness of the Eocambrian evaporates beneath the cover.
3. Reactivation of basement brittle tectonics (more enhanced in the eastern Potwar Plateau).

In Potwar, the EoCambrian evaporate sequence is overlain by Cambrian rocks of Jhelum Group which comprises Khewra Sandstone, Kussak, Jutana, and Bhaganwala Formations. From middle Cambrian to Early Permian the Jhelum group consist of limited deposition or erosion and the strata from these periods are missing in Potwar sub-basin. The continental depositional

environmental of Nilawahan group of early Permian is bounded to the eastern part of Potwar/Salt Range.

According to the interpretation of seismic in structures in Potwar region may be divided into.

- Pop-up anticlines
- Snake head anticlines
- Salt cored anticlines.

### **2.3 Tectonics of Eastern Potwar Basin:**

In the Potwar area, the deformation appears to have occurred by south verging thrusting, with tight and occasionally overturned anticlines separated by broad synclines. The major thrust faults dip to the north and are normally associated with south dipping conjugate back thrusts, which have resulted in the formation of popup structures. The main faults detach on the regional plane of decollement i.e. Salt Range Formation (SRF). The eastern Potwar region represents the most strongly deformed part of the Potwar fold and thrust belt, with large low angle detachment faults accommodating more shortening than elsewhere in the Potwar fold and thrust belt. The area is dominated by over thrust tectonics, where the formations have been compressed into fold and fault dominated structures. In eastern Potwar, most of the folds trend NE -SW, in contrast to the EW trending folds in the central region shown in Fig 2.2. Conventional imbricate thrusts, popup structures, and triangle zones are commonly developed in this area. Over thrusting has produced fault bounded hydrocarbon traps that hold several billions of barrels of reserves? The tectonic framework of the eastern Potwar region is largely controlled by the Salt Range and Domeli fore thrust systems and the Dil Jabba and Domeli back thrusts. The Salt Range thrust (SRT) is an emergent thrust front with a large low angle detachment along which the Potwar Plateau has been translated southward. The Salt Range thrust defines the southernmost boundary of the Potwar area. The Domeli thrust is the second major thrust fault in the eastern Potwar. The Domeli thrust is a foreland verging thrust that shows a significant amount of shortening. The Salt Range thrust is a regional thrust fault and bounds the east west trending mountainous arc and ultimately merges into Jhelum strike slip fault. Paleozoic to Eocene platform series rocks are exposed in the hanging wall whereas Neogene molasses has been extensively under thrust in the footwall of this large over thrust and the Domeli thrust is localized to the region of the eastern Potwar. In the eastern Potwar, some back thrusts are as large as the main thrusts. The Domeli

back thrust is a classic example of a regional back thrust in the eastern Potwar. The Domeli back thrust is interpreted to be a major, late stage feature that developed as a result of the Domeli thrust. No other blind back thrust in any part of the Potwar is larger than the Domeli back thrust. All main faults are sealing as their detachment level is in Precambrian salt (Aamir and Siddiqui, 2006).

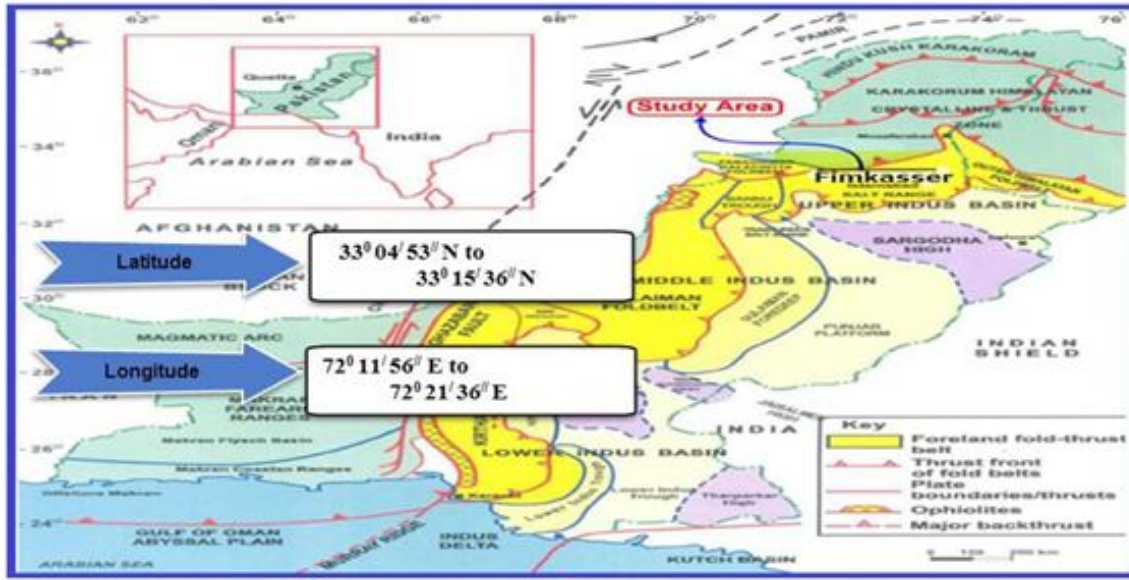


**Figure (2.1): Tectonic map (Banks and Warburton)**

## 2.4 STRATIGRAPHY OF THE AREA:

The stratigraphic column is divided into three unconformity-bounded sequences. These unconformities in the study area are Ordovician to Carboniferous, Mesozoic to Late Permian, and Oligocene in age. The stratigraphic chart is shown in Figure (2.1).

These unconformities are difficult to identify in the seismic profiles due to complicated thrusting. The Potwar sub-basin is filled with thick infra-Cambrian evaporite deposits overlain by relatively thin Cambrian to Eocene age platform deposits followed by thick Miocene-Pliocene molasse deposits. This whole section has been severely deformed by intense tectonic activity during the Himalayan orogeny in Pliocene to middle Pleistocene time. The oldest Formation penetrated in this area is the Infra- Cambrian Salt Range Formation which is dominantly composed of halite with subordinate marl, dolomite, and shale. (Muhammad Aamir and Muhammad Maas Siddiqui, 2006).

The Salt Range Formation is best developed in the Eastern Salt Range. The salt lies unconformably on the Precambrian basement. The overlying platform sequence consists of Cambrian to Eocene shallow water sediments with major unconformities at the base of Permian and Paleocene. The Potwar basin was raised during Ordovician to Carboniferous; therefore no sediments of this time interval were deposited in the basin. The second sudden alteration to the sedimentary system is represented by the complete lack of the Mesozoic sedimentary sequence, including late Permian to Cretaceous, throughout the eastern Potwar area. In Mesozoic time the depocenter was located in central Potwar, whereas thick Mesozoic sedimentary section is present. A major unconformity is also found between the platform sequence and overlying molasses section where the entire Oligocene sedimentary record is missing. The molasses deposits include the Murree, Kamliyal, Chinji, Nagri, and Dhok Pathan Formations (Muhammad Aamir and Muhammad Maas Siddiqui, 2006). Rock units ranging in age from Infra-Cambrian to Cambrian are exposed in the Potwar Province of the Indus basin where the Salt Range Formation with salt, marl salt seams and dolomite is the oldest recognized unit through surface and subsurface geological information and forms the basement for the fossiliferous Cambrian sequence (Shah, 1977). Since the complete section of Salt Range Formation has not been observed in any of the wells of Potwar sub-basin and the Formation is not completely exposed along the Salt Range, it was therefore, assumed in the past that the Salt Range Formation is the oldest rock unit overlying the Pre-Cambrian basement. Extent of these Formations toward north and examination of seismic data indicate that the mentioned Formations may also be present in the eastern Potwar region. The stratigraphy of the area is shown in chart given below in fig 2.1.

## **2.5 PETROLEUM PROSPECT:**

The petroleum prospect of the Area tells us about the source Reservoir and seal Mechanism. The Stratigraphic column of the area shows different rocks act as Source, reservoir and Cap rock in the area. The general description is given below.

### **2.5.1 SOURCE ROCKS:**

Source rock is the productive rocks for hydrocarbons; these rocks also initiate the conversion of organic compound into oil and gas. The Formations which act as source rocks in the study area are as follow.

## **PATALA FORMATION:**

The Patala Formation overlies the Lockhart Formation conformably and its type section is in the Patala Nala in the Western Salt Range (Davies and Pinfold, 1937). It consists largely of shale with sub-ordinate marl, lime stone and sandstone. Marcasite nodules are found in the shale. The sandstone is in the upper part. The Formation also contains coal and its thickness ranges from 27m to over 200m (Warwick, 1990). It contains abundant foraminifera, molluscs and ostracods (Davies & Pinfold, 1937, Eames, 1952, and Latif, 1970). The age of the Patala Formation is Late Paleocene.

## **2.5.2 RESORVOIR ROCKS:**

The main reservoir rocks in the study area are lower Chorgali and Sakesar Formations.

### **SAKESAR FORMATION (EOCENE):**

With increase in limestone beds, the Nammal Formation transitionally passes into the overlying Sakesar Formation, the type locality of which is the Sakesar Peak (Gee, 1935 and Fatmi, 1973). It consists of grey, nodular to massive limestone, which is cherty in the upper part. Near Daudkhel, the Sakesar Formation laterally grades into massive gypsum. Its thickness ranges from 70m to about 450m. Its age is early Eocene.

### **CHORGALI FORMATION:**

The Chorgali Formation rests conformably over the Sakesar Formation (type locality Chorgali Pass) (Pascoe, 1920 and Fatmi, 1973). It consists largely, in the lower part, of thin-bedded grey, partly dolomitized and argillaceous limestone with bituminous odor, and in the upper part, of greenish, soft calcareous shale with inter beds of limestone. It contains molluscs, ostracods and foraminifera.

## **2.5.3 TRAP OR SEAL ROCKS:**

In potwar basin both structural and stratigraphic traps are available. In study area the associated structures are pop up anticlines and snaked head structures. The seal is provided by Murree Formation.



**MURREE FORMATION:**

The Murree Formation of Miocene age provides a lateral and effective seal to reservoir rocks. The Murree Formation consists of clay and shale both of these lithologies act as a good seal rock. The figure (2.2) individually highlights seal, reservoir and source rock encountered in study area.

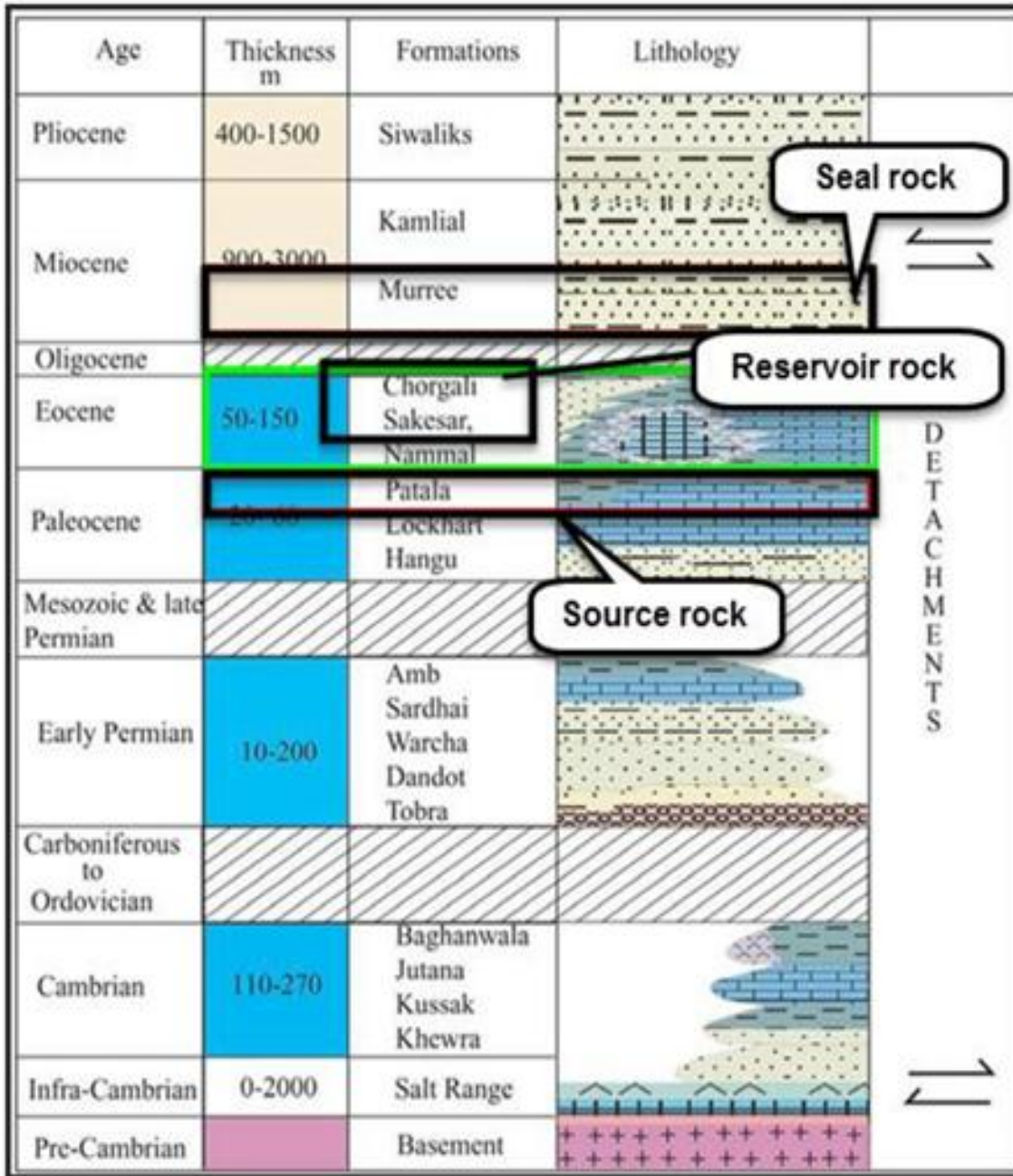


Figure (2.2): Stratigraphic chart of the area. (Aamir and Siddiqui, 2006).

# **Chapter#03**

# **INTERPRETATION OF SEISMIC DATA**

### 3.1 Seismic interpretation:

Seismic interpretation implies picking and tracking seismic reflectors on basis of lateral continuity for the purpose of identifying geologic structures, stratigraphy and petroleum play. The ultimate goal is to portray hydrocarbon accumulation and their extent by keeping economic factor in mind also calculates their volume as well. Conventional seismic interpretation is an art that requires skill and experience in geophysics and geology Badley (1985).

The Seismic data interpretation is the method of determining information about the subsurface of earth from seismic data. It may determine general information about an area, locate prospects for drilling exploratory wells or guide development of an already discovered field (Coffeen, 1986). According to Badley (1985), such reflections and unconformities are to be mapped on seismic section, which fully describe the geology and hydrocarbon potential of the area. If the horizon of interest is not prominent and it is difficult in tracing it over the whole area, it is advisable to pick additional horizons above and or below the target horizon. This helps in understanding the trend and behavior of the target horizon in the zones where its quality is not good enough to be picked with confidence. Final objective of interpretation is conversion of seismic section into a geological section which provides a somewhat realistic subsurface picture of that area, both structurally as well as strati graphically. (Badley, 1985). Flow chart of interpretation is shown in figure 3.1.

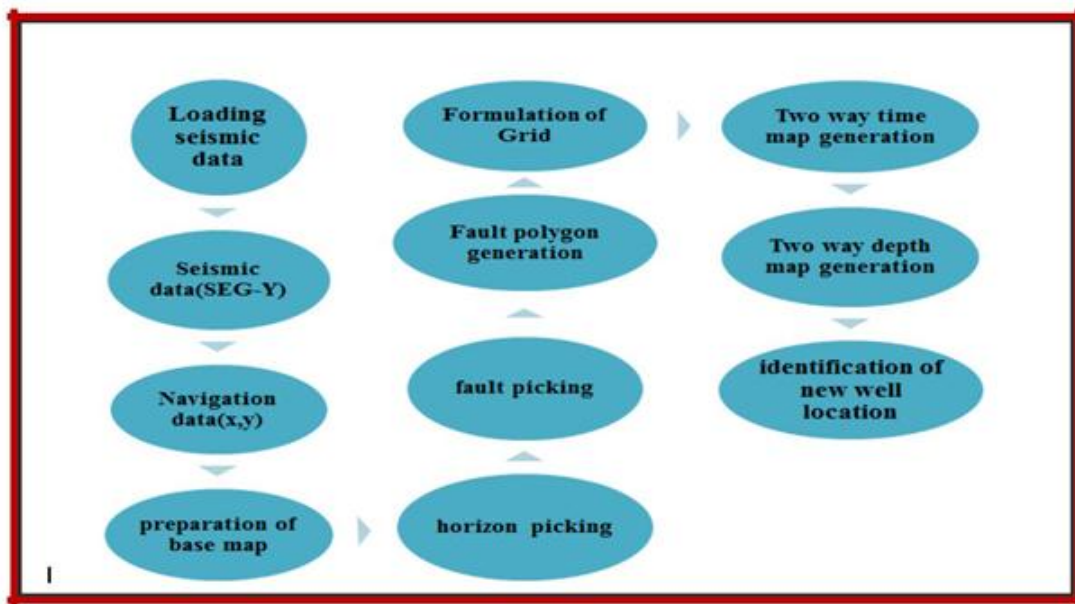


Figure (3.1): Flow chart of Interpretation.

### 3.2 Base map:

Base map is a map which shows orientation and location of the seismic lines and wells. The map consists of dip and strike lines as shown in figure (3.2).

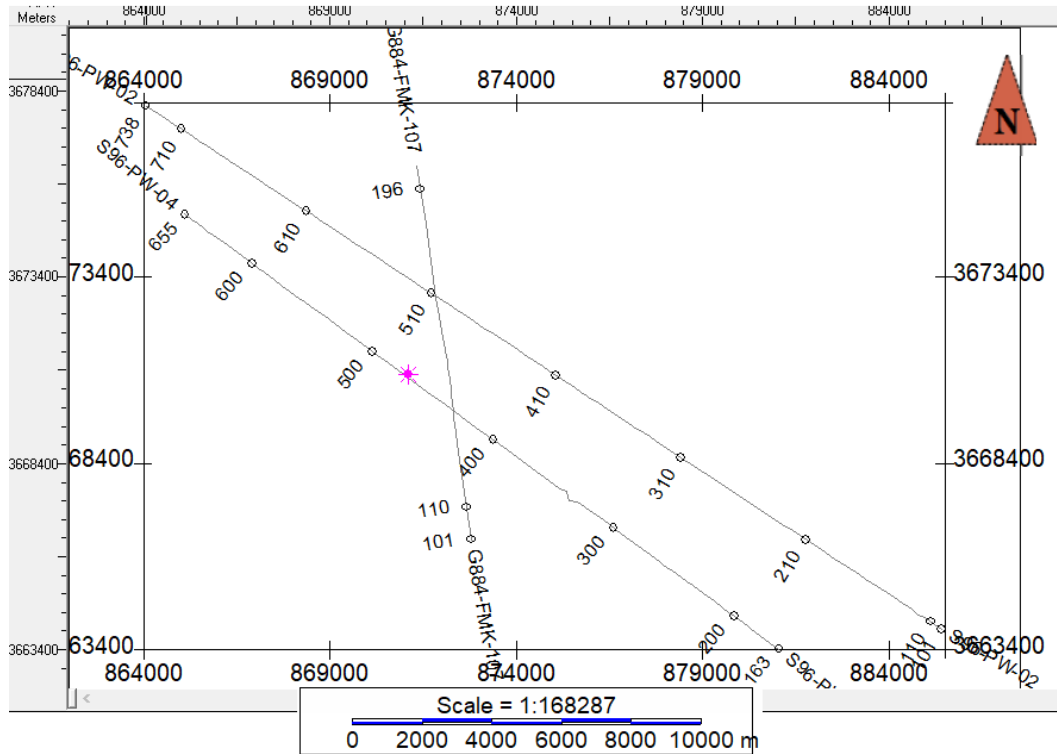
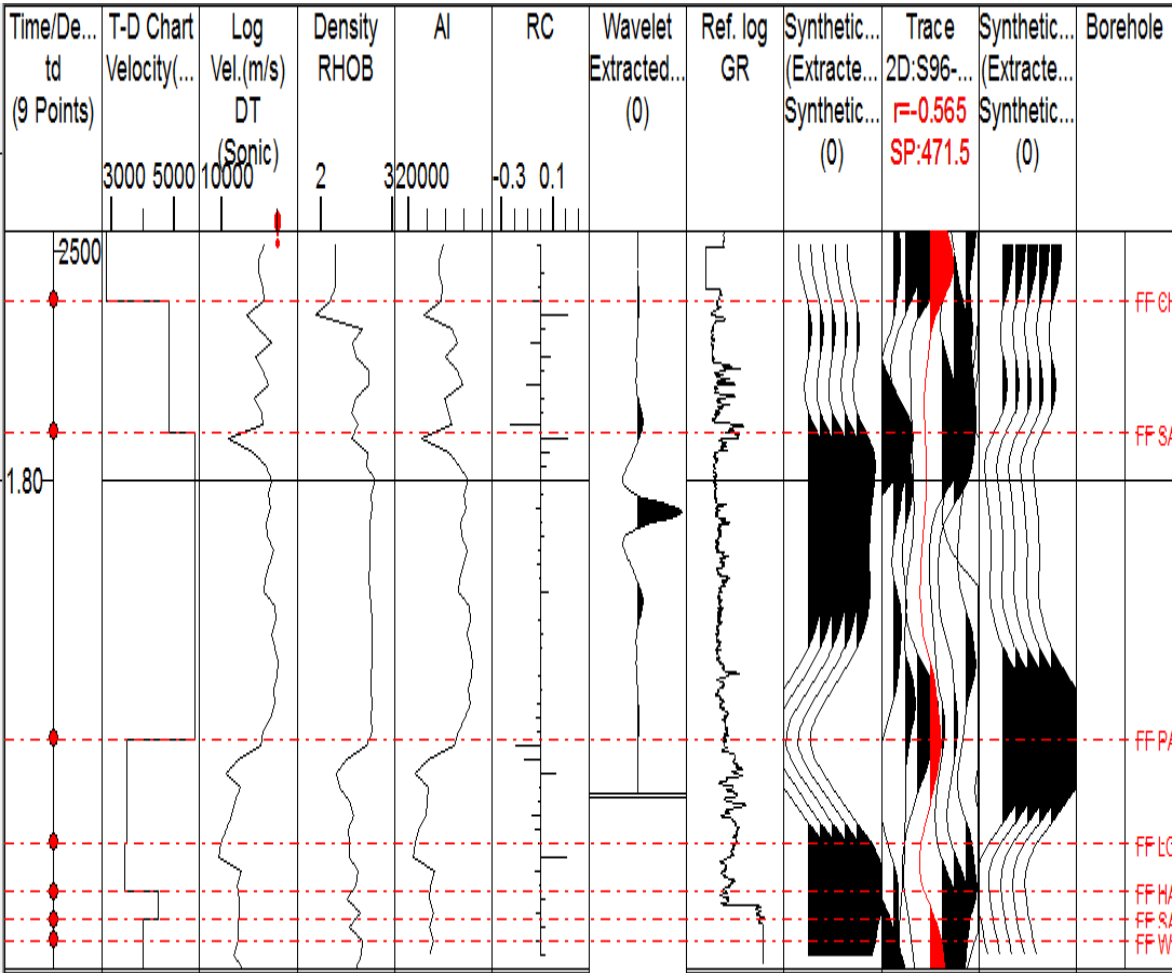


Figure (3.2): Base map of the Fimkassar area.

#### 3.2.1 Generation of Synthetic Seismogram

The more control the geoscientist has in mapping the subsurface, the greater the accuracy of the maps. Control can be increased by the correlation of seismic data with borehole data. The synthetic seismogram is the primary means of obtaining this correlation.

Velocity data from the sonic log (and the density log if available) are used to create a synthetic seismic trace. This trace closely approximates a trace from a seismic line that passes close to the well in which the logs were acquired. The synthetic then correlates with both the seismic data and the well log from which it was generated.



**Figure 3.2.1 Synthetic seismogram of well Turkwall-01**

**3.3 Interpretation of seismic lines:**

It includes following steps.

**Marking Of Seismic Horizons:**

Primary task of interpretation is the identification of various horizons as an interface between geological Formations. For this purpose, good structural as well as stratigraphic knowledge of the area is required (McQuillin, et al., 1984). Thus during interpretation process; I mark both, the horizons and faults on the seismic section. Three horizons are picked on the basis of available information (well data and generalized stratigraphic map). The horizons picked are named on basis of well top of the Turkwal-01 the Chorgali, Sakesar and Patala showing high reflections on a seismic section making it easier to be picked.



### Fault and folds Identification:

To identify faults and folds it is important to have background knowledge about the geology of the area.

### Geology of the Area:

On the basis of the geology of the area, it is evident that the area under study lies in compressional regime. This background knowledge helps us to identify that reverse and thrust faults should be marked on the seismic section.

### 3.4 Interpreted Seismic Sections:

The two dip lines i.e.S96-PW04, S96-PW02 are interpreted are shown in figure (3.3) and figure (3.4) respectively. Three seismic horizons namely; Chorgali, Sakesar of Eocene age and Patala of Paleocene age on the basis of well tops and further more confirmed by synthetic seismogram. Along these seismic horizons three faults are also picked shown in figure (3.3) and figure (3.4).

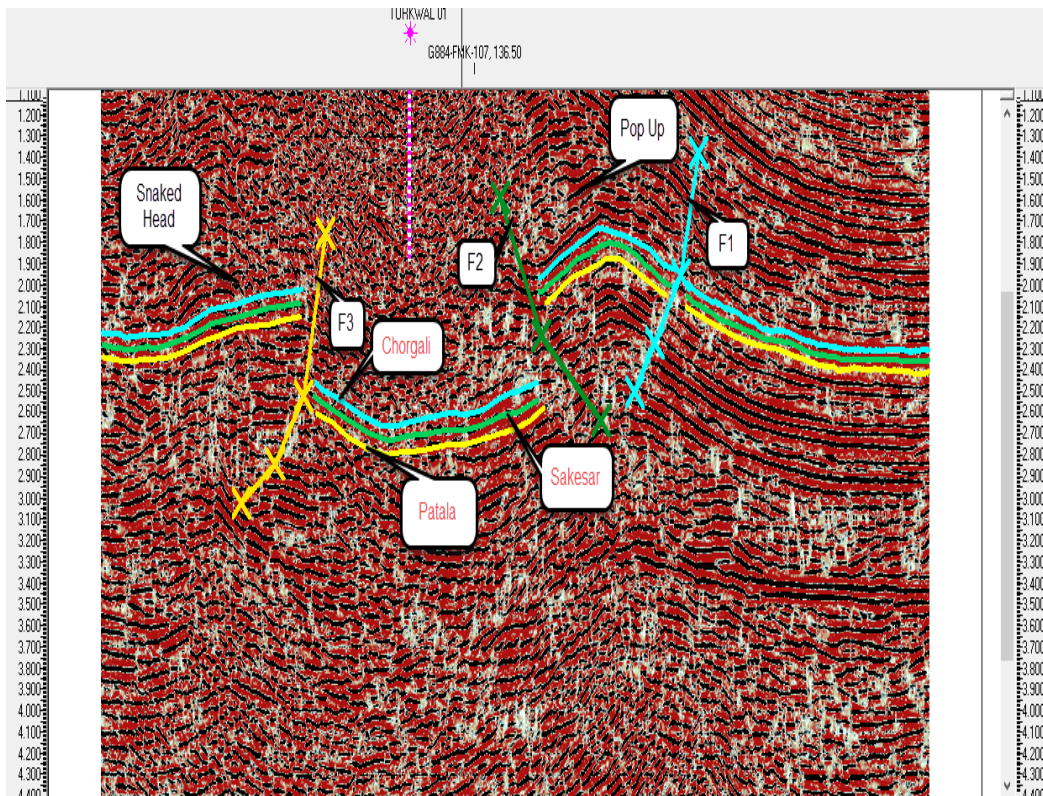
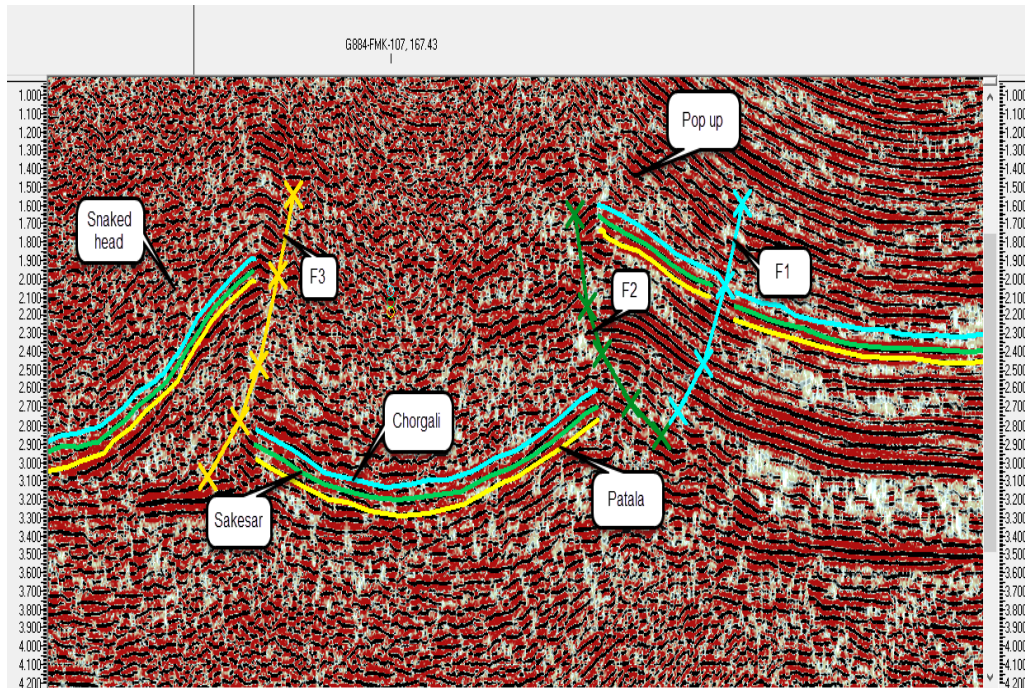


Figure (3.3): Interpreted seismic line PW-04.



**Figure (3.4): Interpreted seismic line PW-02**

### 3.5 Fault Polygons Generation:

Before generation of fault polygons it is necessary to identify the faults and their lateral extent by looking at the available seismic data and assign proper name to all these faults. If one finds that the same fault is present on all the dip lines, then all points (represented by a —+| or —x| sign by Kingdom software) can be manually joined to make a polygon. Construction of fault polygons are very important as far as time and depth contouring of a particular horizon is concerned. Any mapping software needs all faults to be converted in to polygons prior to contouring.

The reason is that if a fault is not converted into a polygon, the software doesn't recognize it as a barrier or discontinuities, thus making any possible closures against faults represent a false picture of the subsurface. After construction of fault polygons, the high and low areas on a particular horizon become obvious. Fault polygons are constructed for all marked horizons and these are oriented in NE-SW 'direction. The fault polygon is shown in figure (3.5).

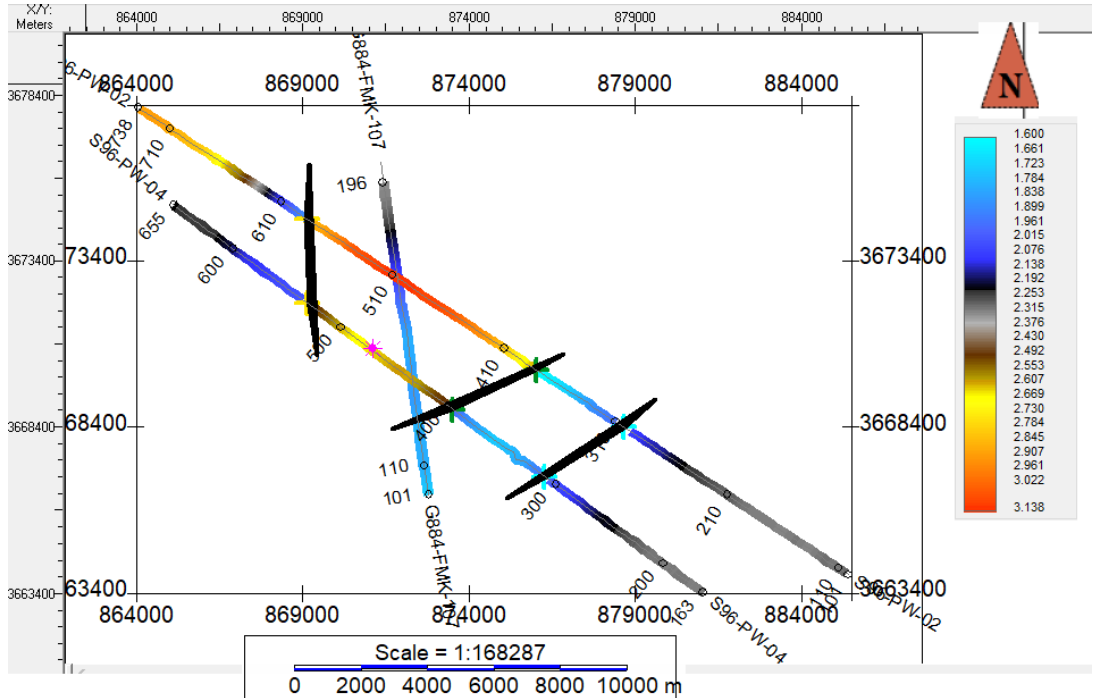


**Figure (3.5): Polygon’s orientation on base map.**

**3.6 Contour maps:**

The results of seismic interpretation are usually displayed in the form of maps. Mapping is part of the interpretation of the data. The seismic map is usually the final product of seismic exploration, the one on which the entire operation depends for its usefulness. The contours are the lines of equal time or depth wandering around the map as dictated by the data (Coffeen, 1986).

In constructing a subsurface map from seismic data, a reference datum must first be selected. The datum may be sea level or any other depth above or below sea level. Frequently, another datum above sea level is selected in order to image a shallow marker on the seismic cross-section, which may have a great impact on the interpretation of the zone of interest (Gadallah & Fisher, 2009).

Contouring represents the 3D earth on a 2D surface. The spacing of the contour lines is a measure of the steepness of the slope i.e. closer the spacing, steeper the slope. A subsurface structural map shows relief on a subsurface horizon with contour lines that represent equal depth below a reference datum or two way time (TWT) from the surface. These contour maps reveal



the slope of the Formation, structural relief of the Formation, its dip, and any faulting or folding. The interpreted seismic data is contoured for producing seismic maps which provide a 3D picture of the various layers within an area which is limited by intersecting shooting lines. The picked times for each reflector is exported along with the navigation data in the form of an XYZ file to be used for contouring.

### **3.7 Time and Depth Contour Maps of Chorgali Formation:**

The time and depth map of Chorgali Formation are generated on the base map along with wells and their corresponding fault polygons shown in figure. The polygon F1, F2, F3 shows dipping in NE-SW direction. The TWT contour map of Chorgali Formation is shown in figure. The contour interval for time contours is set as 40msec and that of depth contour is 80m. The structural variation in these contours is can be interpreted by using color bar and legends. The light orange color from (1.67s-1.882s) shows the shallowest part and light blue color approaches from (2.881s-3.038s) shows the deepest part. The time and depth contour map are shown in figure (3.6) and figure (3.7).

The depth contour map of Chorgali Formation was calculated from the time contour map by using velocity obtained from DT-log run in Chorgali Formation using formula  $S=VT/2$ . The depth variation in contour map is interpreted by using color bar shown in figure. The orange color from (2844m-3035m) shows the shallowest part while light blue color from (4965m-5241m).

The following interpretations are made from these time and depth contours shown in figure.

- The interpreted structure for Chorgali Formation is a pop-up anticline and snaked head structure.
- The pop up anticline is bounded by thrust faults F1 and F2 and snaked head structure is formed due thrust fault F3. The time and depth contour map are shown in figure (3.6) and figure (3.7)

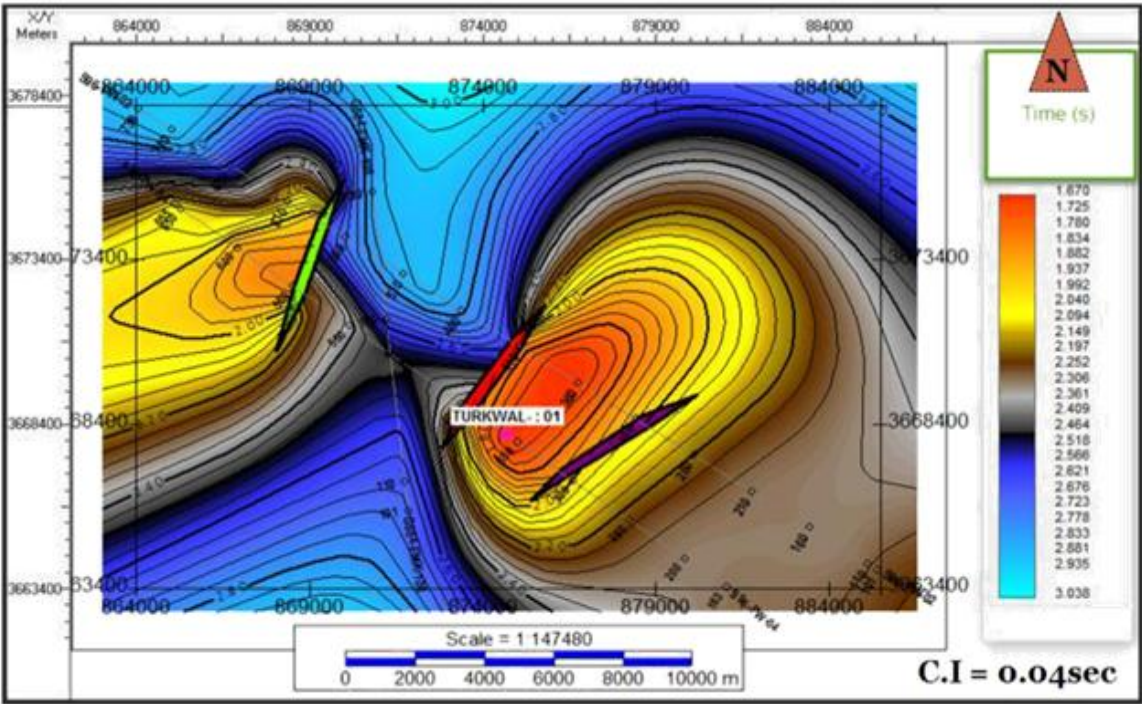


Figure (3.6): TWT contour map of Chorgali Formation.

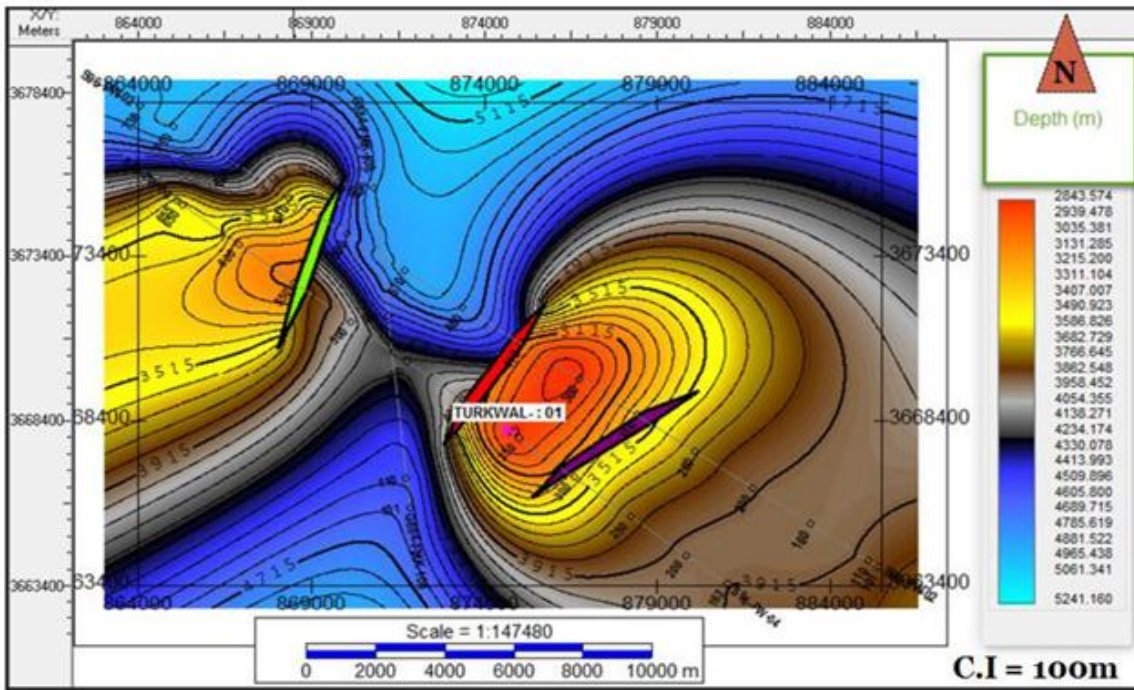


Figure (3.7): Depth contour map of Chorgali Formation.

### 3.8 Time and depth contour map of Sakeser Formation:

The time and depth map of Sakeser Formation are generated on the base map along with wells and their corresponding fault polygons shown in figure. The polygons F1, F2, F3 are dipping in NE-SW direction. The TWT contour map of Chorgali Formation is shown in figure. The contour interval for time contours is set as 40ms and that of depth contour is 100m. The structural variation in these contours can be interpreted by using color bar and legends the light blue color ranges from (1.753s-1.934s) shows the shallowest part and yellow to orange color approaches from range (3.018s-3.019s) shows the deepest part. The contour map helps us to mark the zone of interest and gives hint about the location of second well. Sakeser Formation is the second zone of interest and one of the major potential reservoirs after Chorgali. Here at this level similar fault polygon are observed which indicates a presence of same faults on both Formations. Hence blue color ranges from (1.753s-1.843s) shows the highest peak or elevated part i.e. most favorable area for hydrocarbon extraction. Time and depth contour map of Sakeser Formation are given below in fig (3.8) and fig (3.9).

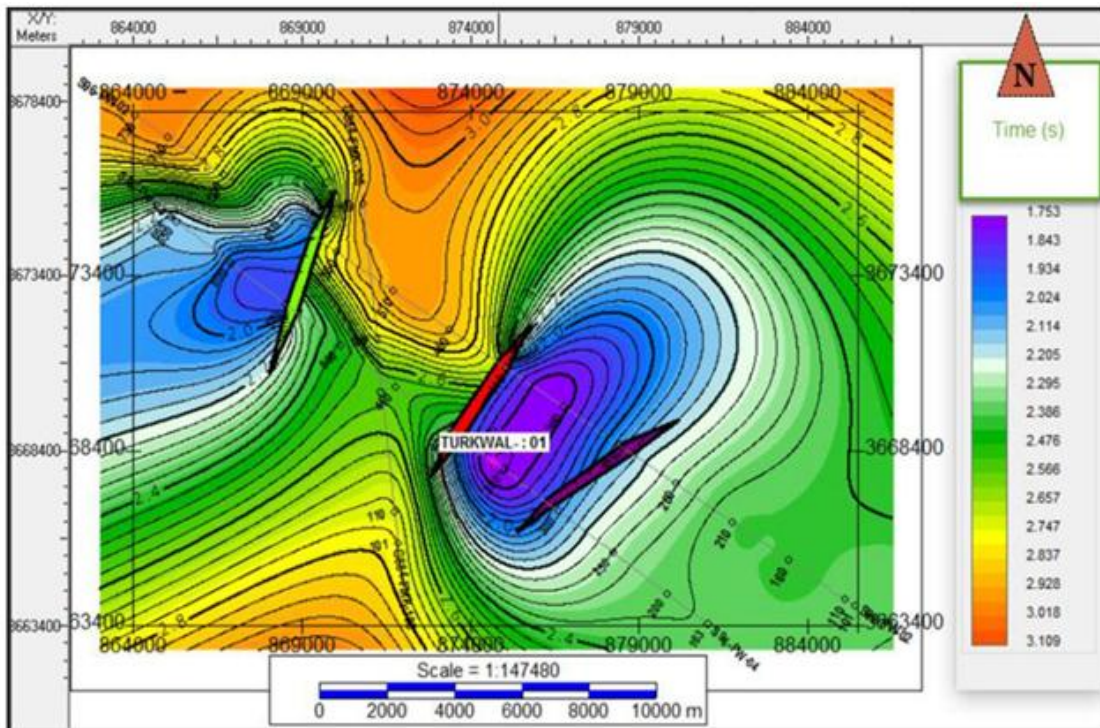
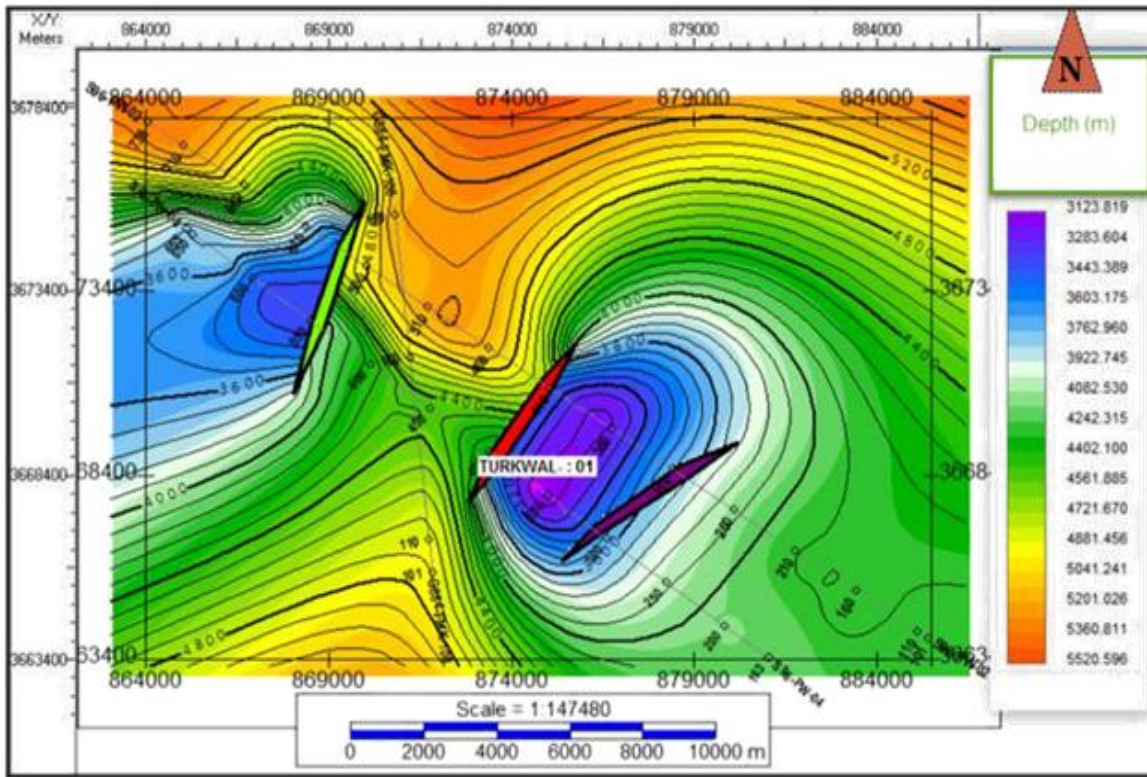


Figure (3.8): TWT contour map of Sakeser Formation.





**Figure (3.9): Depth contour map of Sakesar Formation.**

### **3.9 Time and depth contour of Patala Formation:**

Patala Formation can act as both reservoir as well as source rock. The time and depth contour map is generated can be interpreted as by two other Formations using color bar. The time and depth maps can be interpreted by using same techniques as we have done in previous Formations. The contour map shown in figure almost gives same structure interpretation as of previous two Formations discussed above. The time and contour maps of Patala Formation is shown in figures (3.10) and (3.11) below.

The TWT contour map can be interpreted from the color bar. The light blue color shows the shallowest part or elevated part is our zone of interest ranges from (1.82s-2.116s). It is interpreted as pop-up structure because value of time is decreasing as we move outward. The depth map of Patala Formation is also constructed by same procedure that we have discussed above. The depth map of Patala Formation can also interpreted by using color bar. The depth value ranges from (3123.519m-3427.091m) shown by blue light blue color and purple color (5351m-5520m) represents the deeper part.

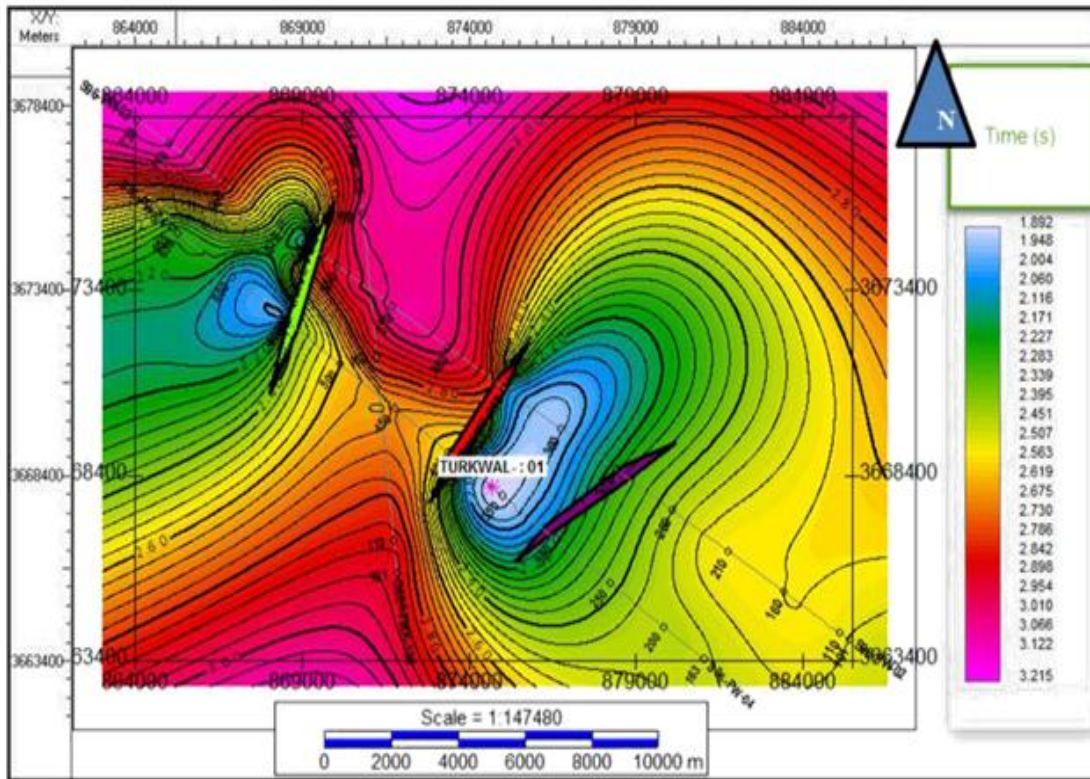


**Figure (3.10): TWT contour map of Patala Formation.**

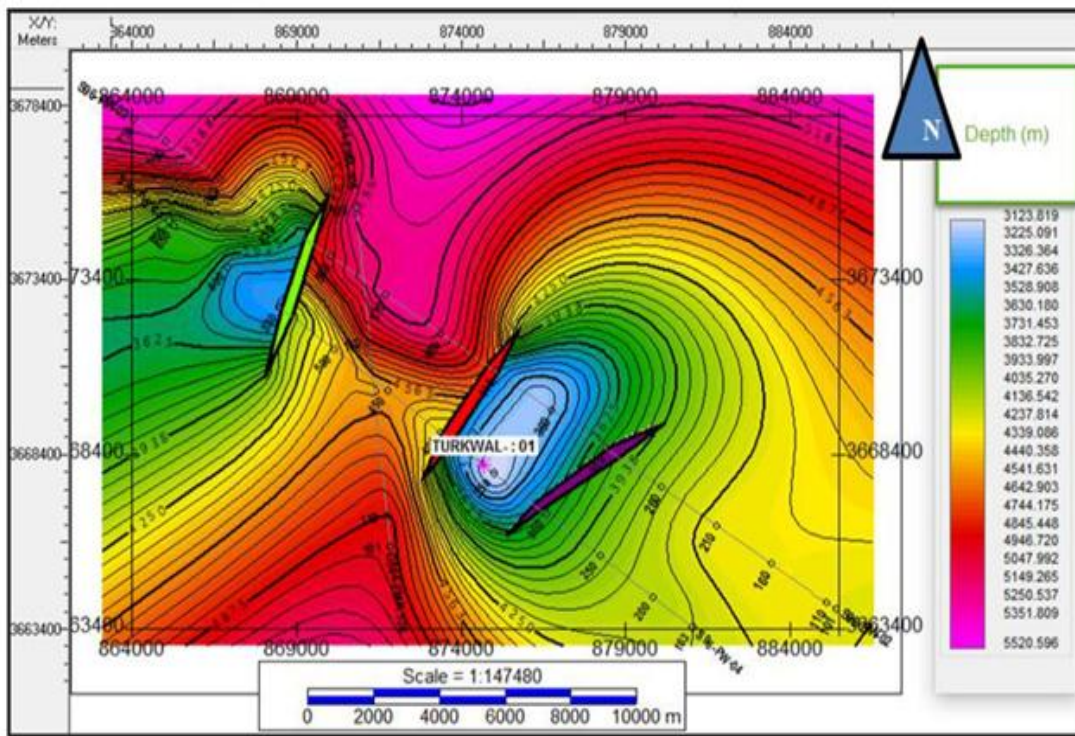


**Figure (3.11): Depth contour map of Patala Formation.**



### 3.10 Identification of well location:

The purpose of generating contour map is to find to determine the area where hydrocarbons accumulate. The hydrocarbon mostly accumulates in the regions of low pressure and permeability. Ideally these regions are hinge of the anticlines. In real case the hinge of anticline are also structurally disturbed and there is a risk of drilling in that location (Coffeen, J.A., 1986). So there arises a need of detailed study of the area. The petroleum play of Fimkassar area consist of Murree Formation as seal rock, Chorgali Formation as reservoir rock and Patala act as both source and reservoir rocks. The pop-up anticline structure is associated with thrust faults and other faults in adjacent area provide low pressure areas, so may be marked as proposed possible well locations. The locations are identified over depth contour maps illustrated below in figure.

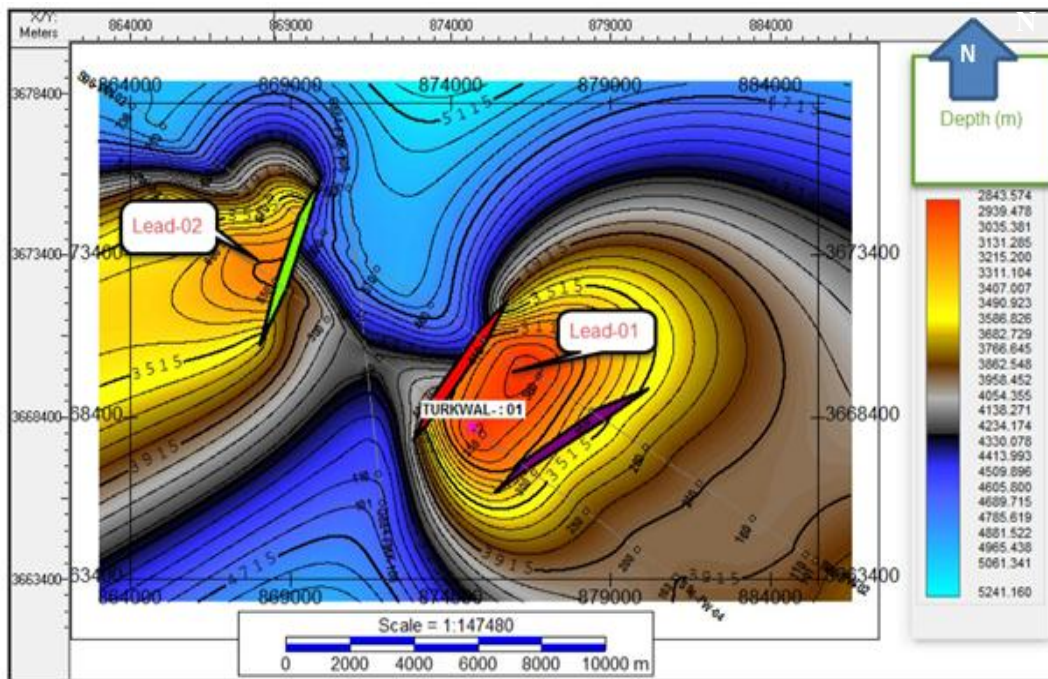


Figure (3.12): Identification of leads of Chorgali Formation.

#### 3.10.1 Lead-01:

This lead is marked on the closure formed near the undulating hinge line of the subsurface Fimkassar anticlinal structure as shown in figure. The may be formed because of folding and faulting and subsurface topography. On time contour map of Chorgali Formation lead is marked by (1.834s) and on depth map it is marked by (3035m), at Sakesar Formation it is marked by (1.753s) and on depth contour map it is marked by(3300m) and at Patala Formation (2.004s).

### 3.10.2 Lead-02:

The lead is a three way dip structure comprised of snaked head structure shown in figure. Two sides of closure is controlled by thrust fault and third side is controlled by dip of the structure This lead represents time (1.834s) at Chorgali in fig, Sakesar at (2.024s) and Patala Formation at time (2.062s). Lead-01 and lead-02 are shown is figure (3.12), (3.13), (3.14) for Chorgali, Sakesar and Patala Formations respectively.

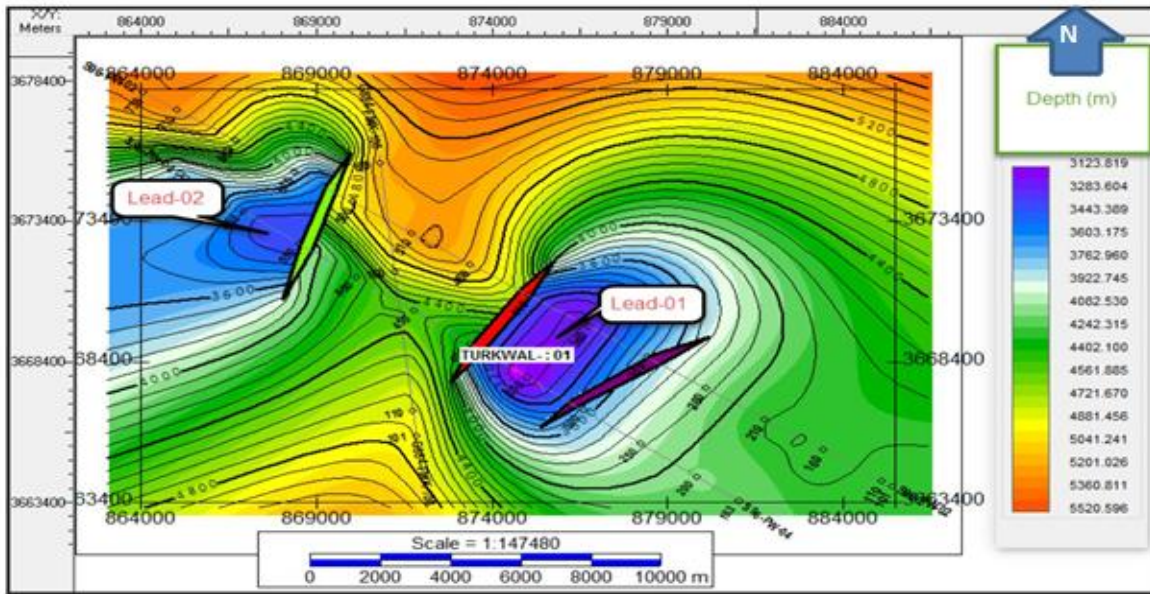


Figure (3.13): Identification of Leads of Sakesar Formation.

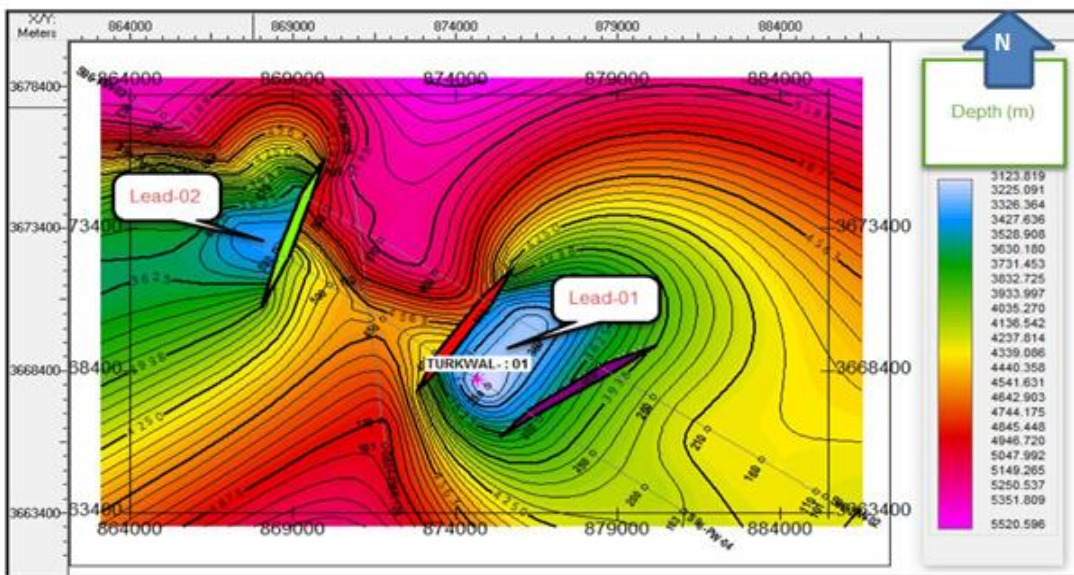


Figure (3.14): Identification of Leads of Patala Formation.

# **Chapter#04**

# **PETROPHYSICS**



## **4.1 Introduction:**

This study facilitates in identification and quantification of fluid in a reservoir (Ali et al., 2014). Knowledge of reservoir physical properties like volume of shale, porosity, and water and hydrocarbon saturation is needed to define accurately probable zones of hydrocarbons. The physical property like volume of shale, porosity, saturation of water and saturation of hydrocarbon is needed to identify the probable zones of hydrocarbons accurately. The combination of petrophysics with rock physics enables the geophysicists to understand the physical properties of rocks in the study area. Petrophysics is apprehensive with using well measurements to subsidize reservoir depiction (Daniel, 2003). . To accurately characterize oil or gas in a reservoir, measurements such as resistivity, porosity and density are made, from which volume of shale, average porosity water saturation and hydrocarbon saturation can be quantified.

## **4.2 Petrophysical analysis:**

The petrophysics analysis has been carried out in order to measure the reservoir characterization of the Fimkessar area using the borehole data of Turkwal-01. We used the log curves including spontaneous potential log (SP), Gamma ray (GR), Sonic log (DT), Latero log deep (LLD), Latero log shallow (LLS), Neutron log, density log, Photo electric effect log (PEF).For petrophysics analysis the following parameters are calculated for reservoir rock.

- Volume of shale (by Gamma ray log)
- Porosity of reservoir (by SONIC, DENSITY and NEUTRON logs)
- Water saturation (by LLD, LLS and SP logs)
- Hydrocarbon Saturation (HCS)
- Permeability of reservoir rock (Ross Willey equation)

## **4.3 Estimation of volume of shale:**

The volume of shale can be estimated from the response of Gamma ray log. The response of Gamma ray must be known through different lithologies. The gamma ray log is the passive logging because we measure the Formation properties without using any source. Actually it is the measures the Formation's radioactivity. The gamma ray emits from the Formation in the form of the Formation in the form of the electromagnetic energy which are called the photon. When photon collides with the Formation electron hence they transfer the energy to the

Formation electron so the phenomenon of the Compton scattering occurs. Now these emitted Gamma rays reached to the detector of the gamma ray and counted and displayed as count per second which is termed as the Gamma ray. The volume of the shale is calculated by using (Asquith and Gibson, 2004) equation given below.

$$\text{IGR} = \frac{\text{GR}_{\text{log}} - \text{GR}_{\text{max}}}{\text{GR}_{\text{max}} - \text{GR}_{\text{min}}}$$

**GR (max)** = 100% shale.

**GR (min)** = 0% shale or clean Formation.

The Gamma ray log shows maximum value when shale is encountered and shows a minimum value when clean lithology like sand is encountered. These values are calculated from given log response and then volume of shale is estimated by using (Asquith and Gibson, 2004) equation. The volume of shale calculated in Turkwal – 01 well located in Fimkassar area is 47%.

#### **4.4 Estimation of porosity:**

Porosity is the ratio of volume of voids to total volume of rock. Porosity is calculated for different zones of interest by using the following logs, sonic log, neutron log, density log.

##### **4.4.1 Calculation of porosity from sonic log:**

Sonic log device consists of a transmitter that emit sound waves and a receiver that picks and record the compressional waves as it reach the receiver. This log is a recording verses depth of time (t) which is required by a compressional wave to go across 1 feet of Formation, called interval transient time  $\Delta t$ , while it is the reciprocal of the velocity of sound wave. This time ( $\Delta t$ ) is depended upon lithology and porosity of the Formation (Asquith and Gibson, 2004). Sonic log can also be used for the following purposes in combination of other logs as given by (Daniel, 2004).

Sonic log is also used in with combination with other logs to achieve our desired goals. The various combinations are given below.

- a. Lithology identification (with neutron or density).
- b. Synthetic seismogram (with density).
- c. Mechanical properties of Formation (with density).

The mathematical relation used for calculating the porosity from sonic log is written be

$$\phi_s = \frac{\Delta t_{log} - \Delta t_{mat}}{\Delta t_{fl} - \Delta t_{mat}}$$

The interval transient time of Formation increased due to presence of hydrocarbon known as hydrocarbon effect. This effect should be removed because it affects the values of calculated porosities.

#### 4.4.2 Calculation of porosity from density log:

In the density logging gamma ray collide with the electron in the Formation and scattered gamma ray (Compton scattering) received on the detector which indicate the density of the Formation increase in the bulk density of the Formation causing the decrease in the count rate and vice versa. Bulk density which is obtained from the density log is considered the sum of the density of the fluid density and the matrix density of the Formation.

If rock type is known then porosity is calculated by using (Asquith and Gibson, 2004) equation. The rock lithology is known by using gamma ray log in this case it is limestone. The following relation is used for calculating porosity.

$$\phi_d = \frac{\rho_m - \rho_b}{\rho_m - \rho_f}$$

$\phi_d$ = Density Log porosity

$\rho_m$ = Density of matrix ( limestone= 2.7 )

$\rho_b$ = Bulk density of formation

$\rho_f$ = Density of fluid ( salt mud = 1.1, Fresh mud = 1 )

### 4.4.3 Calculation of porosity from neutron log:

This is the type of porosity log which measure concentration of Hydrogen ions in the Formation. Neutron is continuously emitted from chemical source in the tool of the neutron logging. When these neutron collide with nuclei in the Formation and results in loss of some energy. Hydrogen atom has same mass as that of neutron, maximum loss of energy occurs when electron collides with hydrogen atoms.

Hydrogen is an indication of the presence of the fluid in the Formation pores; hence loss of energy is related to the porosity of the Formation.

The neutron porosity is very low when the pores in the Formation are filled with the gas instead of the water and oil; the reason is that gas having less concentration of the hydrogen as compared to water and oil. This less porosity by the neutron PHI due to the presence of the gas called the gas effect (Asquith and Gibson, 2004).

### 4.5 Total porosity:

The total porosity is the sum of all the porosities calculated from different logs divided by the number of logs used for calculating porosities. The total porosity is calculated for the reservoir which is Chorgali in this case. The mathematical relation is used for this purpose is given below.

$$\varphi_T = \frac{\varphi_d + \varphi_n + \varphi_s}{3}$$

$\Phi_{\text{total}}$  = Average porosity

### 4.6 Estimation of water saturation:

Water saturation is the percentage of pore volume in rock that is occupied by water of Formation. If it is not confirmed that pores in the Formation are filled by hydrocarbons, it is assumed that these are filled with water. To determine the water and hydrocarbon saturation is one of the basic goals of well logging. To calculate saturation of water in the Formation, a mathematical equation was developed by Archie shown below. All the parameters of Archie equation can be calculated from resistivity and spontaneous potential logs.

$$S_w = \left( \frac{R_w * F}{R_t} \right)^{1/n}$$

$R_w$  = Resistivity of water

$R_t$  = True resistivity

$F$  = Formation factor ( $F = \left(\frac{a}{\phi m}\right)$ )

$n$  = Saturation exponent (value varies between 1.8 to 2.5)

$\phi$  = Effective porosity

$m$  = Cementation factor constant = 2

$a$  = 1

All the parameters of Archie equations are calculated by using different various logs discussed below.

#### **4.6.1 Estimation of true resistivity:**

Basically there are different types of electrical Resistivity Logs. But in my work I have only two logs available in my data which are simply explained as follow. These logs are used to measure the resistivity of the subsurface, but actually they measure the resistivity of the Formation fluids. They are very helpful in order to differentiate between water filled Formation and the hydrocarbon filled Formations. Resistivity logs include the following.

- Laterolog Deep (LLD).
- Laterolog shallow (LLS).

#### **Laterolog Deep (LLD):**

Latero log deep is used for the deep investigation of the quietly undisturbed (Uninvaded zone) and it is called Laterolog deep (LLD). This log is also used for saline muds also in case of fresh mud. This log is generally used for measuring the Formation resistivity. It has deep penetration as compared to the (LLS).

#### **Laterolog Shallow (LLS)**

Laterolog shallow (LLS), used for shallow investigation of the transition zone / invaded zone. The depth of the investigation is smaller than the LLD.

These logs are used to calculate the true resistivity.

## 4.6.2 Estimation of resistivity of water:

The resistivity of water is calculated by Spontaneous potential log. The steps are discussed below

The steps are discussed below

1. Pick SSP from S-P log by using formula given by (Rider, 1996)

$$\mathbf{SSP = SP_{clean} - SP_{shale}}$$

SSP = Static spontaneous potential.

SP Clean= Spontaneous potential for sand.

SP Shale= Spontaneous potential for shale.

The value of SSP in OXY-01 is calculated to be -19 mv.

2. Determine the Formation temperature TF against the depth (d) using formula shown in equation given by (Rider, 1996).

$$T_f = \frac{d(BHT - T_s)}{T_D + T_s}$$

D =Depth of Formation (3250m).

T<sub>f</sub> = Borehole temperature (820F).

T<sub>s</sub> = Temperature at surface (260F).

T<sub>D</sub> = Temperature at depth.

3. Resistivity of the mud filtrate is calculated 0.48Ωm at surface temperature by using this relation.

$$R_{mf} = R_{mfe} \left( \frac{T_s + 6.67}{F_t + 6.67} \right)$$

Where,

T<sub>s</sub> = Surface temperature

R<sub>mfe</sub> = Resistivity of mud filtrate equivalent.

F<sub>t</sub> = Formation temperature.

4. Now resistivity of the mud equivalent (Rmfeq) is calculated by using Schlumberger chart shown in figure (4.1).

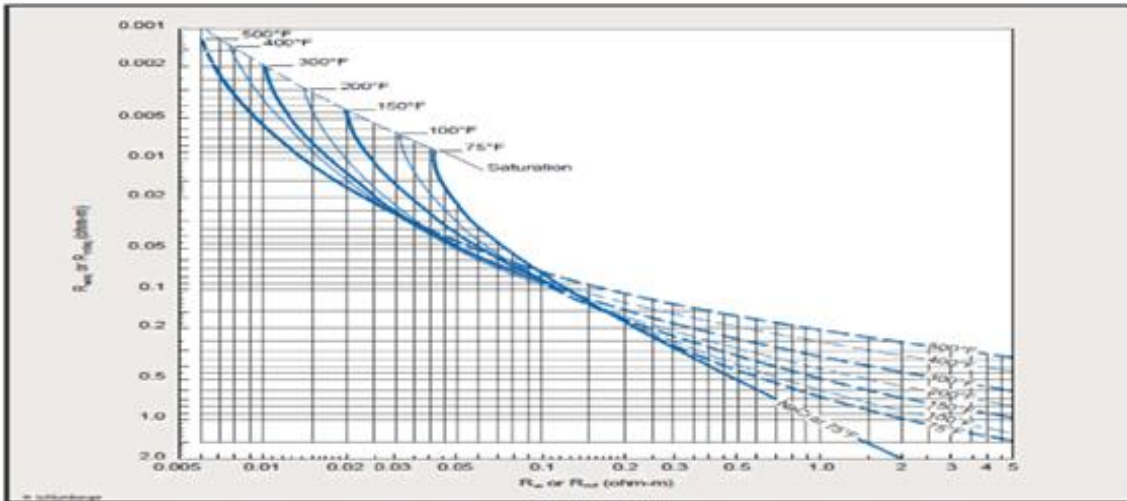


**Figure (4.1): Determination of Rweq from SP chart (Schlumberger, 1989).**

5. Rweq (Water equivalent resistivity) is determined from the Essp (Static spontaneous potential).
6. This is the last step in this step the value of the resistivity of the water (Rw) is obtained against the value of the Rweq (Resistivity of the water equivalent) and Formation temperature.

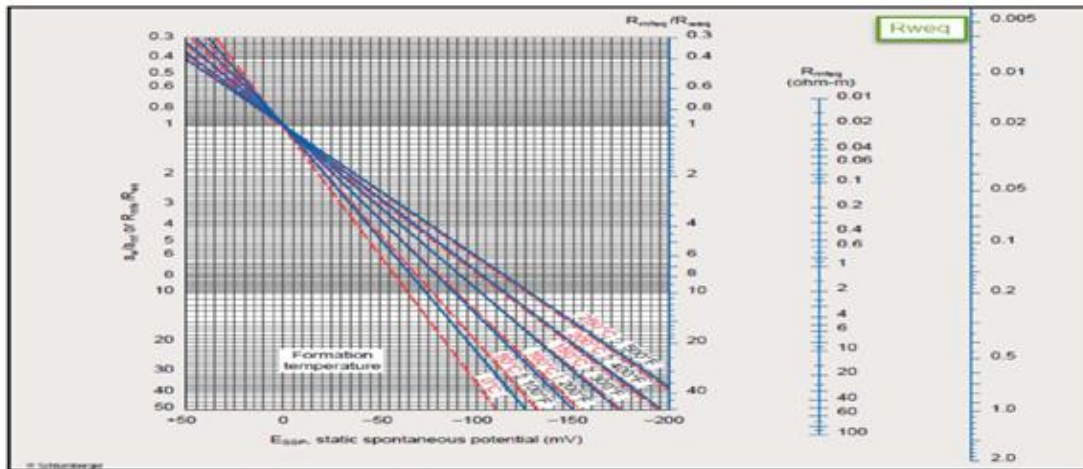


**Figure (4.2): Determination of Rw from SP chart (Schlumberger, 1989)**

The resistivity of water calculated is  $0.042\Omega\text{m}$  for Chorgali and  $0.049\Omega\text{m}$  for Sakesar. After calculating all these parameters we use Archie equation for calculating saturation of water stated below.

$$S_w = \left( \frac{R_w * F}{R_t} \right)^{1/n}$$

#### **4.7 Estimation of hydrocarbon saturation:**

The fraction of pore spaces containing hydrocarbons is known as hydrocarbon saturation. The simple relation used for this purpose is given below.

$$S_w + S_H = 1$$

The saturation of hydrocarbons is percentage of pore volume occupied by hydrocarbon.

Where,

$S_H$  = Hydrocarbon saturation and

$S_w$  = Water saturation

#### **4.8 Well log interpretation of turkwal-01:**

The interpretation of turkwal-01 is shown in figure given below. The Chorgali Formation is encountered at the depth ranges from (2800m-3000m). The Chorgali Formation is confirmed as a reservoir by different results obtained from well log. The Chorgali Formation is encountered at ideal depth which is required for hydrocarbon accumulation. The other logs like Gamma ray log shows low value of Gamma ray readings and resistivity logs shows high values. The volume of shale is far less than 50%. The neutron log shows good porosity values and density and sonic logs shows low values as well. These results are satisfactory thus we can interpret that Chorgali act as a reservoir.



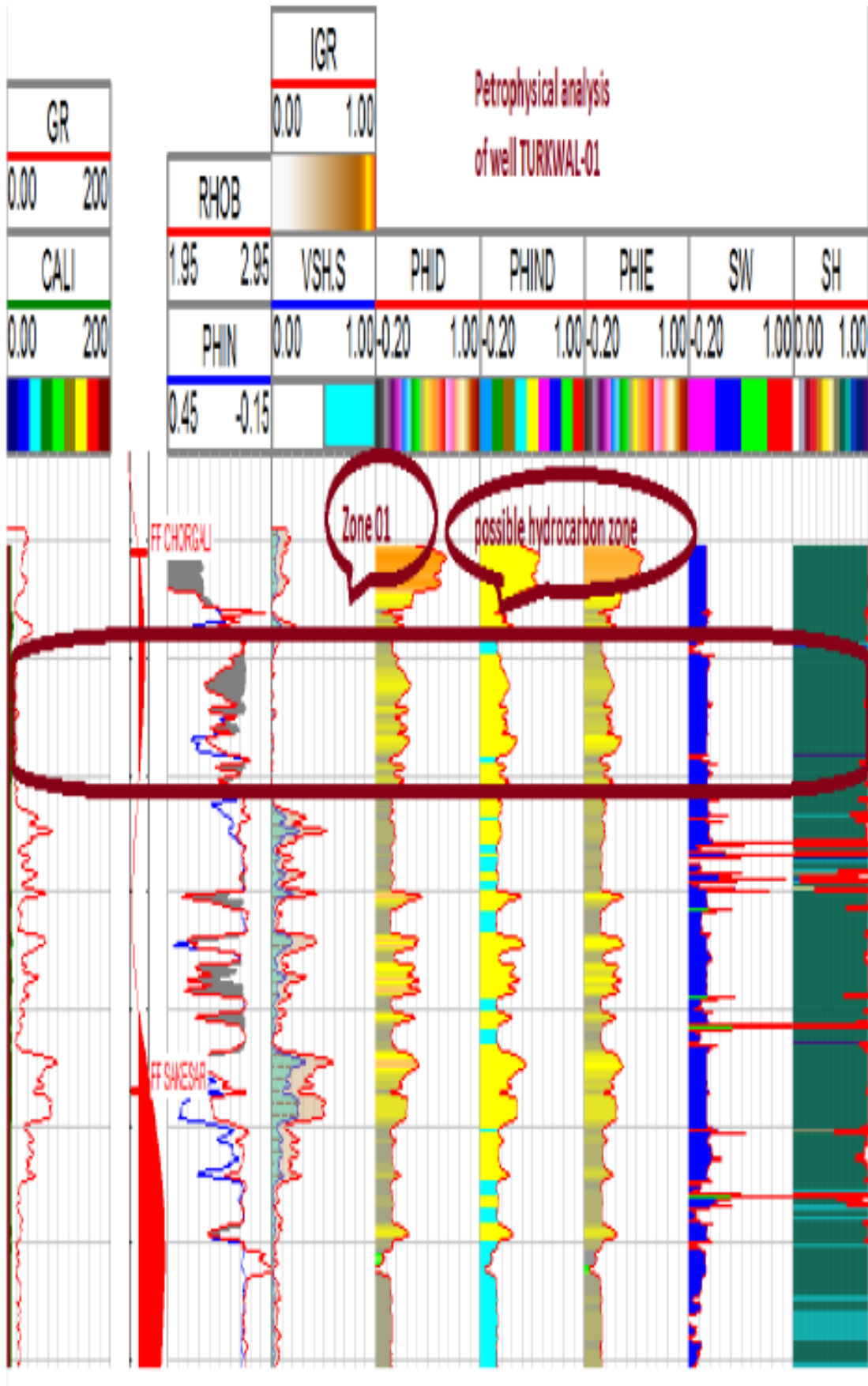


**Figure (4.3): Petrophysical analysis of Chorgali Formation in well Turkwal-01.**

The possible hydrocarbon zone is shown by a rectangle of red color.

**Chorgali Formation (Turkwal-01) results based on well logging interpretation:**

Average volume of shale = 35%.

Total porosity = 20%.

Average water saturation = 41%.

Permeability of reservoir rock = 641 Milli Darcy.

Average hydrocarbon saturation = 59%

**4.9 Cross- plot of neutron and density log:**

When any two values are cross plotted, the resulting series of points shows the relationship between these two variables, or define fields, using both x and y axis values and gives the both upper and lower limits of both variables (Rider 2002). There are some types of well-logs cross plots exist

- Cross-plots of compatible logs: Cross plot between those logs measures the same parameter. For example neutron porosity vs. density porosity logs.
- Cross-plot of incompatible logs: Cross plot between those logs does not measures the same parameters e.g. plot between RHOB, LLD and GR

The typical cross-plot uses an average fluid and rock parameters and would produce lithology behavior. This cross-plot is based on the density response equation where,

$$\rho_b = \rho_{ma} + (\rho_f - \rho_{ma})\phi_N$$

$\rho_b$  = Bulk density.

$\rho_{ma}$  =Matrix density.

$\rho_f$  = Fluid density.

$\phi_N$  = Neutron porosity.

The density log is plotted on x-axis and neutron log is plotted on y-axis and gamma ray values as scale. As this is compatible plot thus it measures a same parameter. There are three lithologies are shown lime stone, dolomite and sand stone. The blue dots represent limestone. The other two lithologies are almost absent in this case. This is because the values of logs used are obtained only from reservoir. The reservoir is Chorgali and it is limestone it confirms our interpretation.

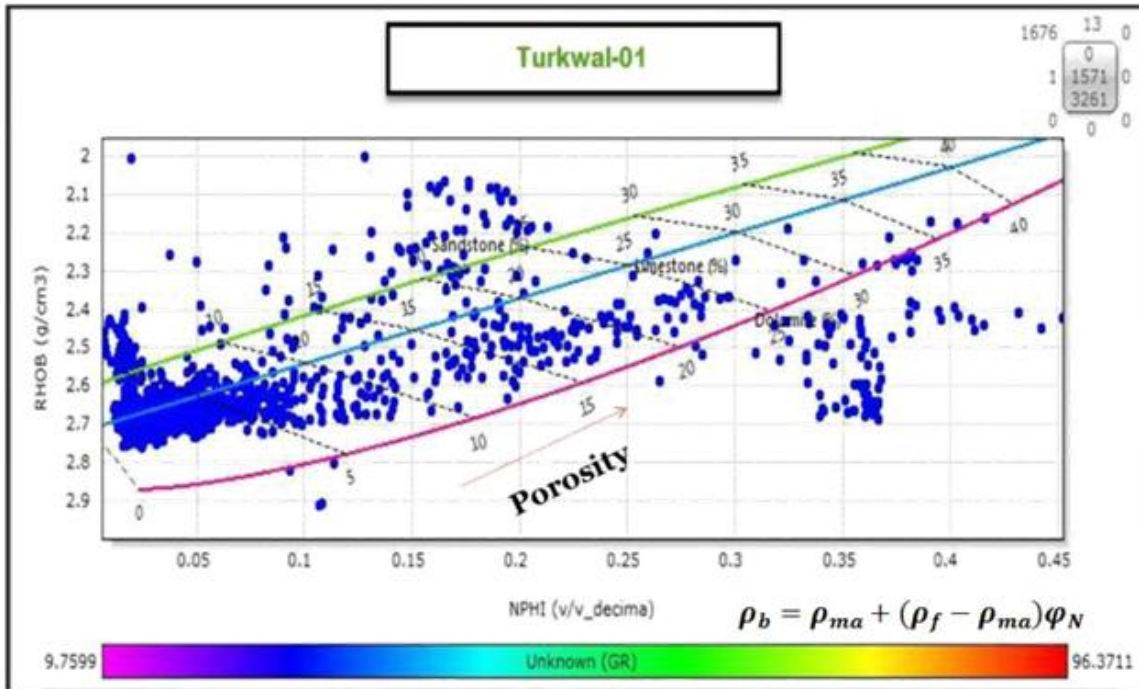


**Figure (4.4): Cross plot of RHOB vs. NPHI using GR as color code for Chorgali Formation in Turkwal-01.**

# Chapter#05

## COLORED INVERSION OF POST STACK DATA

## 5.1 Wavelet and acoustic impedance:

For many seismic processing applications, it becomes necessary to derive an estimate of the seismic wavelet. Because the character of wavelet is imprinted on seismic traces, it is important to understand its shape in order to decipher the properties of earth's interior from seismic traces. In spite of the fact the wavelet is time varying and is expected to be spatially varying, an overall knowledge of wavelet is crucial to enhancing resolution for better imaging of structure and predicting lithology and fluid content. The most common practice is to invert post-stack seismic data for wavelets. A post-stack trace emulates a zero-offset or normal-incidence seismogram, which can be simulated using convolution model assuming 1D earth model. Most seismic data contain noise this problem must be compensated.

In frequency domain, the convolution operation is replaced by a multiplication. Three inverse problems are identified.

- Estimation of the wavelet when the reflection co-efficient is known.
- Estimation of reflection co-efficient or acoustic impedances when the wavelet is known.
- Simultaneous inversion for acoustic impedance of wavelet.

Inversion of seismic data to Acoustic Impedance is usually seen as a specialist activity, so despite the publicized benefits, inverted data are only used in a minority of cases. To help overcome this obstacle we aimed to develop a new algorithm which would not necessarily be best in class, but would be quick and easy to use and increase the use of inversion products with in BPA. This new technique, Colored Inversion, performs significantly better than traditional fast-track routes such as recursive inversion, and benchmarks well against unconstrained sparse-spike inversion.

Once the Colored Inversion operator has been derived it can be simply applied to the data on the interpretation workstation as a user-defined filter. In this way inversion can be achieved within hours since the volume data do not have to be exported to another package, and no explicit wavelet is required. The inversion is understood simply by this flow chart.

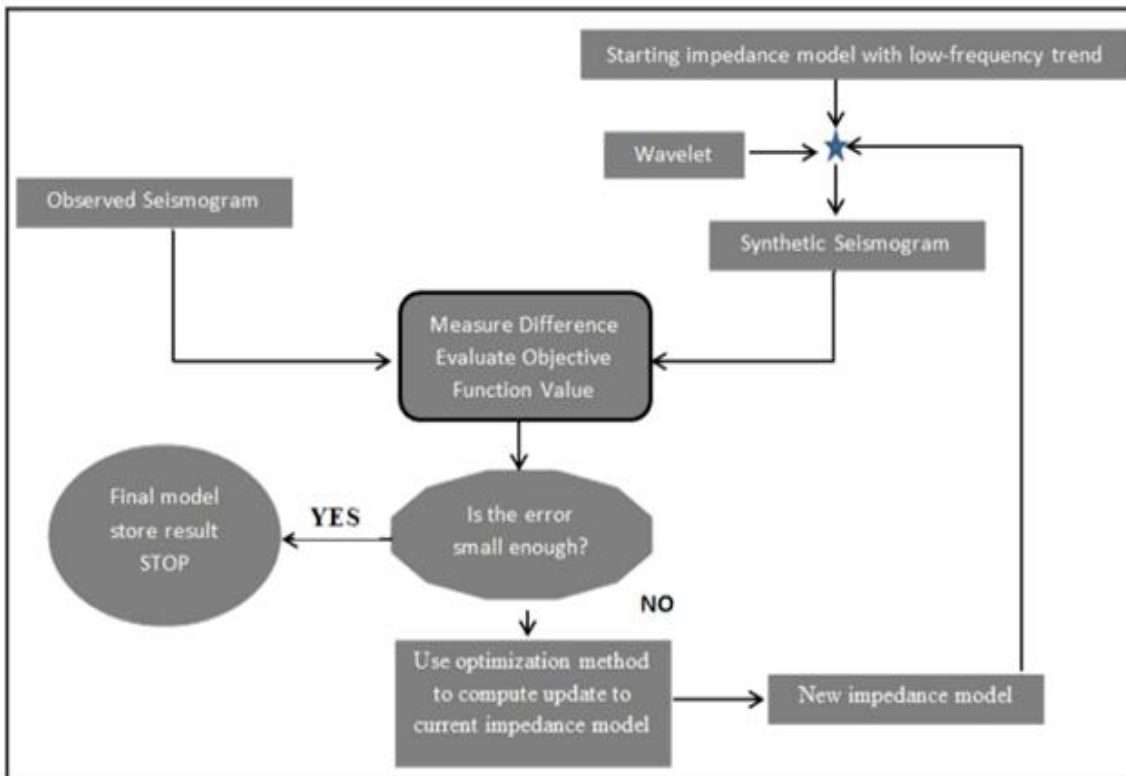


**Figure (5.1): A flow chart showing impedance and wavelet extraction scheme.**

## 5.2 Methodology:

The well data and information of logs is required for the performing the colored inversion in

Kingdom Software.

- The velocity is obtained from sonic log and density is obtained from density log and values of densities are obtained from density log by convolving these values.
- We get acoustic impedance by cross-matching these impedance data with the input reflection data.
- We derive a single optimal matching filter Figure (5.8). Convolving this filter with the input data we see in figure (5.7) that the result is very much similar, everywhere.
- This Empirical observation indicates that inversion can be approximated with a simple filter and that it may be valid over a sizeable region.

The phase of the operator is a constant  $-90^{\circ}$  which is in agreement with the simplistic view of inversion being akin to integration, and the concept of a zero-phase reflection spike being transformed to a step AI interface, provided the data are zero-phase.

Walden & Hoskins's (1984) empirical observation tells us that earth reflection coefficient series have spectra that exhibit a similar trend that can be simply described as constant function. The term is a positive constant and as frequency arrives at a similar observation theoretically may vary from one field to another but tends to remain reasonably constant within any one field (Velzeboer 1981).

It therefore follows that if our seismic data are inverted correctly they too should show the same spectral trend as logs in the same area.

### **5.3 Non uniqueness and convolution:**

The process of convolution for constructing a seismogram using a wavelet and acoustic impedance is performed to generate an operator. Note that wavelet is smoothly varying function, while the reflectivity is a series of delta functions placed at two-way normal time of each reflector (Cooke and Schneider 1983). The spectra of the wavelet and reflectivity series for synthetic are also shown in figure. We observe that wavelet is a band-limited, while reflectivity series is a broad-band. Because the convolution is equivalent to multiplication in frequency domain the spectrum of resulting seismogram is band-limited as well. We can imagine the complexity of the problem further we can take into account the loss of high frequencies of wavelet caused by attenuation. In other words series cannot be assumed to be stationary. Even under stationary conditions the data does not contain all the frequencies. The most common approach to deriving the wavelet is based on well-log data that produce a true reflectivity series.

### **5.4 Wavelet extraction:**

The wavelet is shown in figure (5.2) is extracted on the basis of the well log data that provides the true reflectivity series (i.e. compressional wave velocity and density computed into acoustic impedance logs, which are mapped into normal incidence reflectivity series). An initial guess of wavelet is convolved with reflectivity series and synthetic normal incidence trace is generated. The difference between the observed and synthetic traced is minimized using a suitable chosen norm with smoothness constraints (Mrinal K. Sen).

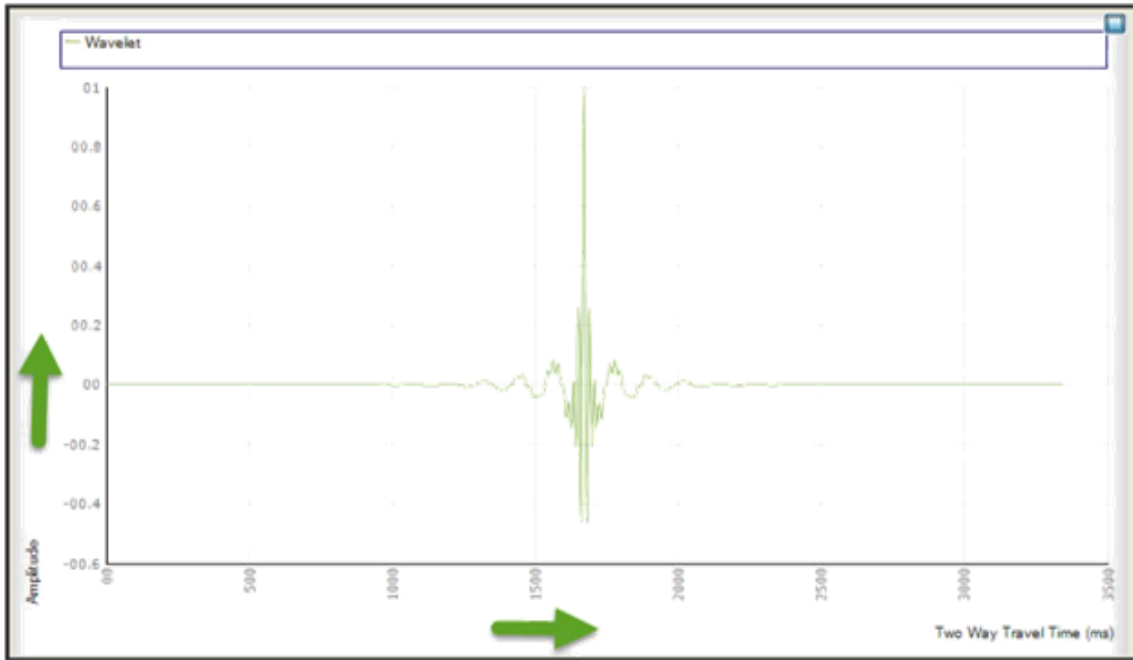


**Figure (5.2): Extracted Wavelet**

### 5.5 Impedance estimation:

Now our approach is to convolve this wavelet with acoustic impedance (reflectivity series). The acoustic impedance is also computed from well log data as described previously. The impedance spectrum is shown in figure (5.3) is estimated after removing source wavelet; noise must be absent; all multiple reflections must be removed; spherical spreading including all plane reflections (Ghosh 2000).

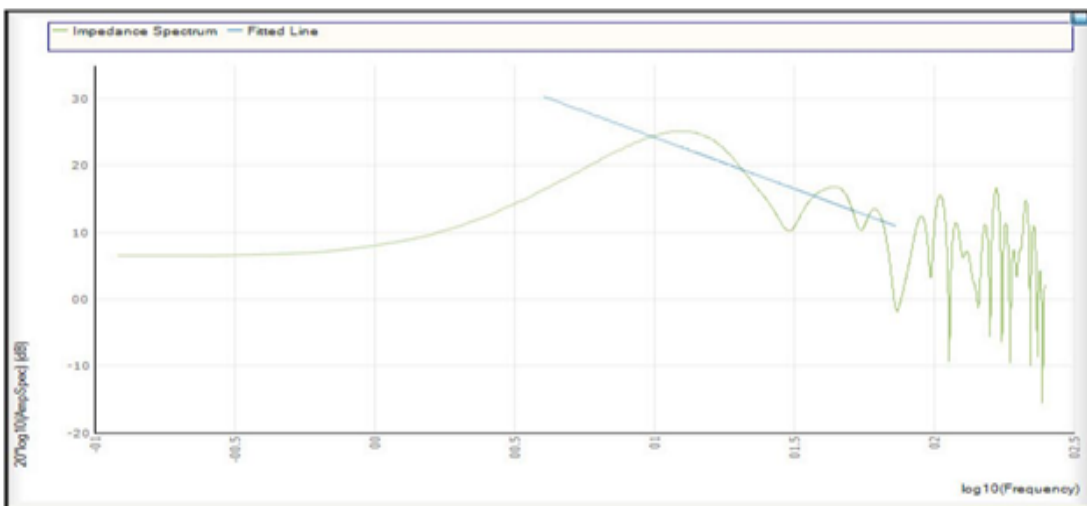


**Figure (5.3): Impedance spectrum with fitted line.**



## 5.6 Butterworth filter:

The Butterworth filter is a type of signal processing filter designed to have as flat a frequency response as possible in the pass band. It is also referred to as a maximally flat magnitude filter. It was first described in 1930 by the British engineer and physicist Stephen Butterworth in his paper entitled "On the Theory of Filter Amplifiers."

An ideal electrical filter should not only completely reject the unwanted frequencies but should also have uniform sensitivity for the wanted frequencies. This filter is used here for convolution of the wavelet and reflectivity series for formulation of seismogram. The Butterworth filter is shown in figure (5.4).

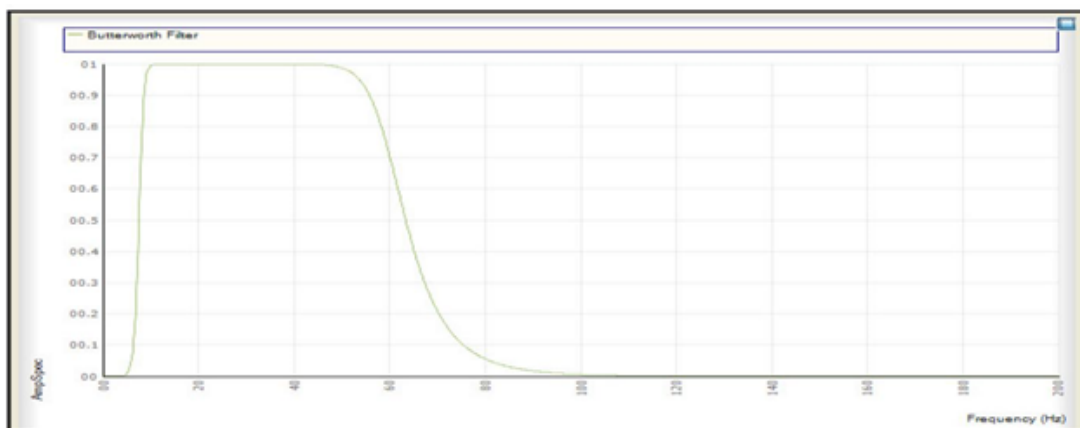


**Figure (5.4): Butterworth filter.**

After the process of convolution is performed we get the seismogram (operator). There is a vast difference between the seismogram of our desire and the seismogram we obtained from the convolution.

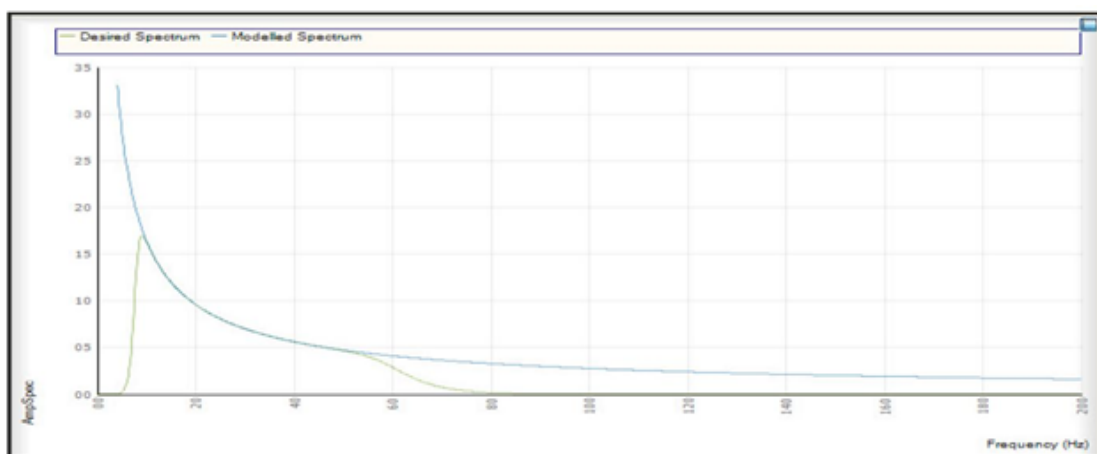


**Figure (5.5): Desired and modeled spectrum.**

There are two spectrums shown in figure (5.5) both are of different colors. The blue color shows the spectrum obtained from convolution of wavelet and acoustic impedance and the spectrum in blue color shows a desired spectrum. Now we need to obtain a spectrum of our desire for this purpose we have to convolve this spectrum with another spectrum known as shaping spectrum which is obtained by applying Fourier transformation on desired spectrum. The shaping spectrum is shown in figure (5.6).

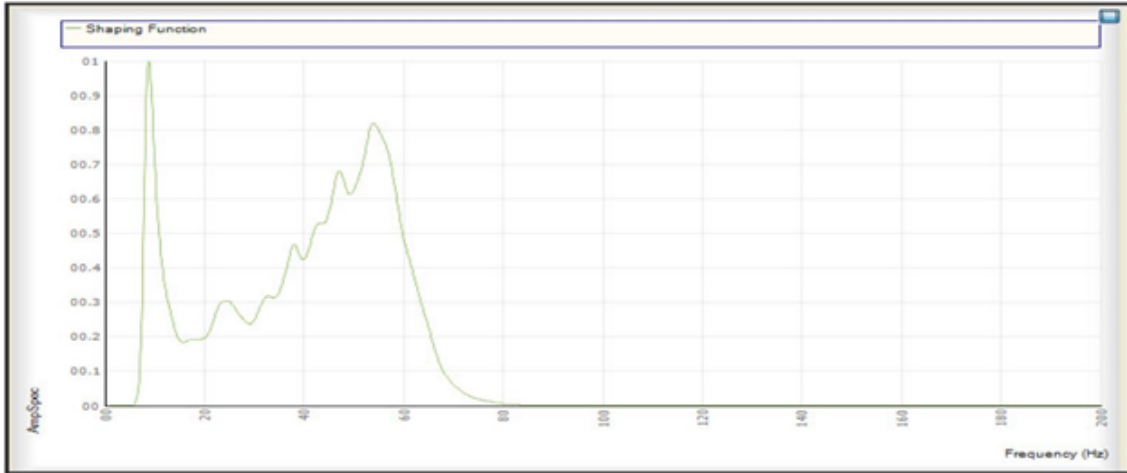


**Figure (5.6): Shaping spectrum.**

The figure (5.6) shows us the shaped seismic spectrum and desired seismic spectrum.

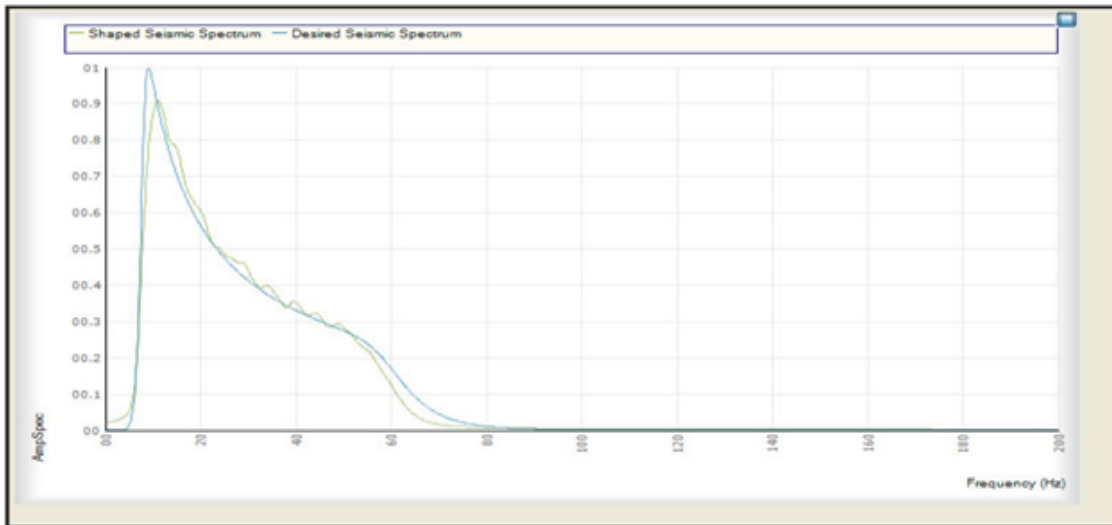


**Figure (5.7): Convolution of shaped seismic spectrum and desired spectrum.**

A seismogram for specific window (as values of acoustic impedance is obtained from well data) is developed now we develop a seismogram to invert whole section. For this purpose we convolve desired spectrum with seismic mean spectrum. After convolving seismogram with

seismic mean spectrum we are able to apply it on whole seismic section. The figure 5.8 shows seismic mean spectrum and desired spectrum.

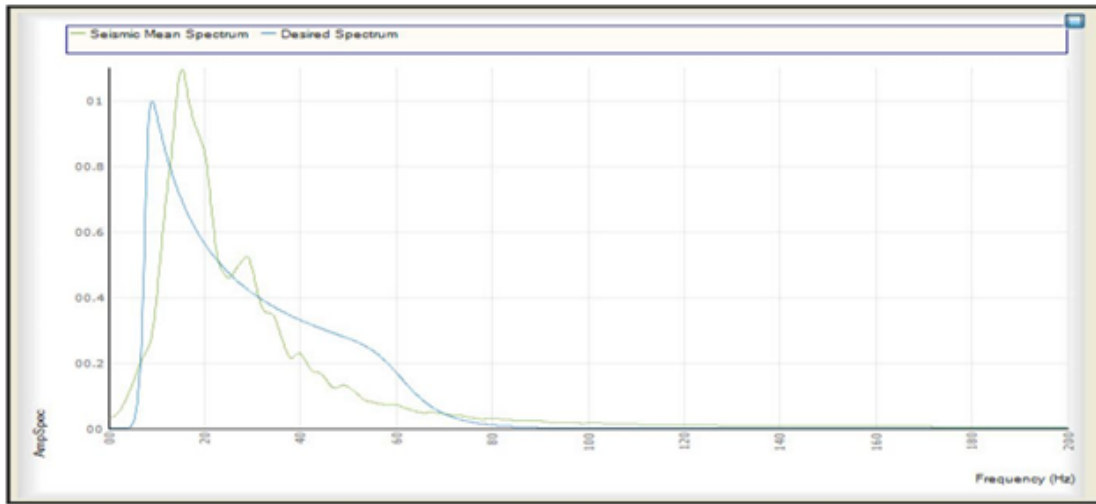


**Figure (5.8): Convolution of seismic mean spectrum and desired spectrum.**

After completion of the process of generating synthetic seismogram, the section is inverted and an acoustic impedance is shown on section instead of amplitude as shown in figure (5.9).

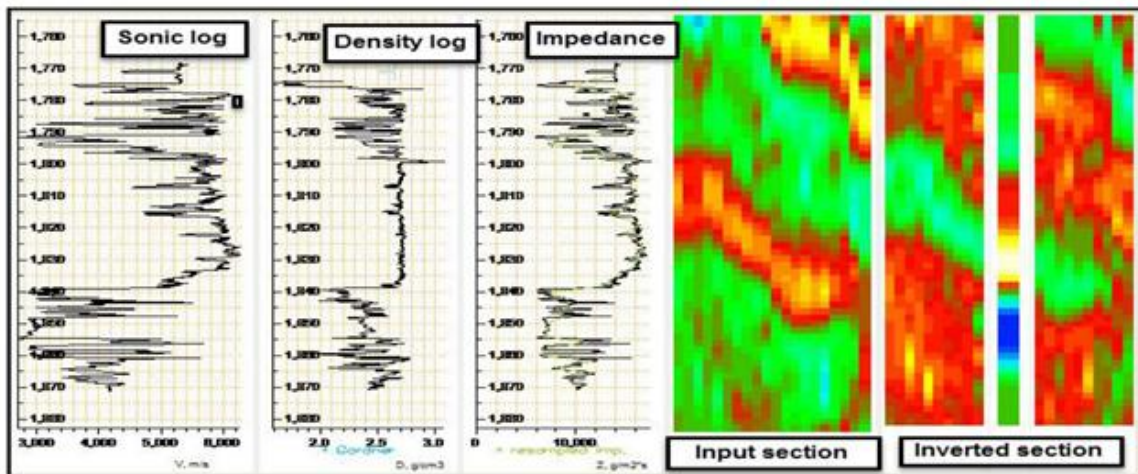


**Figure (5.9): Input seismic section and inverted section along with logs.**

This window displays sonic log and density logs. These logs are used to compute the acoustic impedance. If values of density log are missing then Gardner equation is used to estimate these densities. This equation is very popular in petroleum exploration because it can provide information about the lithology from interval velocities obtained from data these values are calibrated from sonic and density well log information but in the absence of these, Gardner's

constants are a good approximation for density. At the right corner of the window input seismic section is shown on left side and inverted section is shown on the right hand side. The inverted section is shown on the both sides of logs sides of the well the log is inverted to invert the seismic section.

The zoomed picture of inverted section is shown in the figure (5.10) given below.

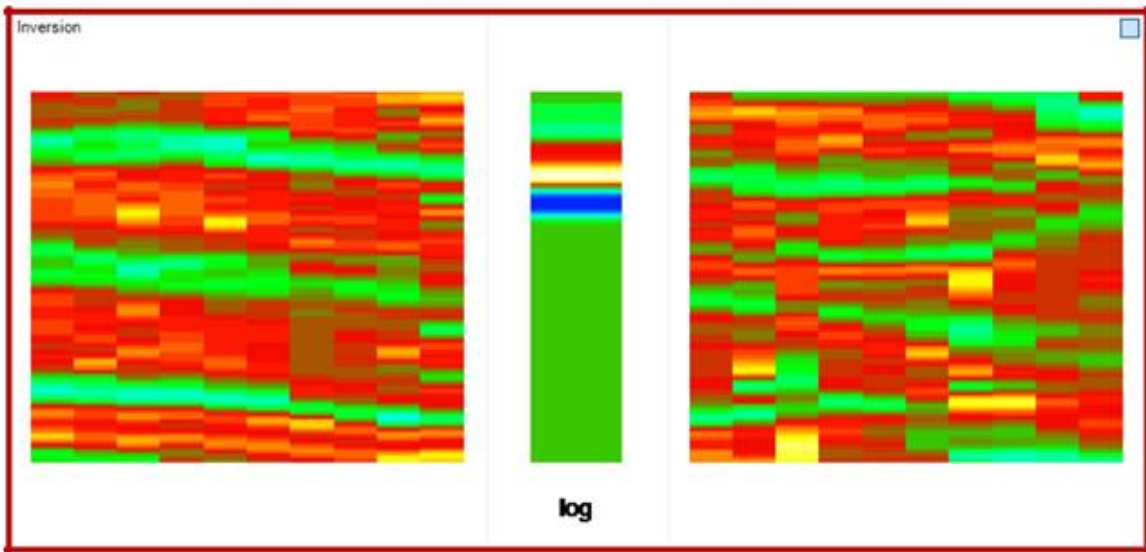


**Figure (5.10): Inverted section with inverted Logs**

Now inversion is applied to the whole section shown in figure 5.11.

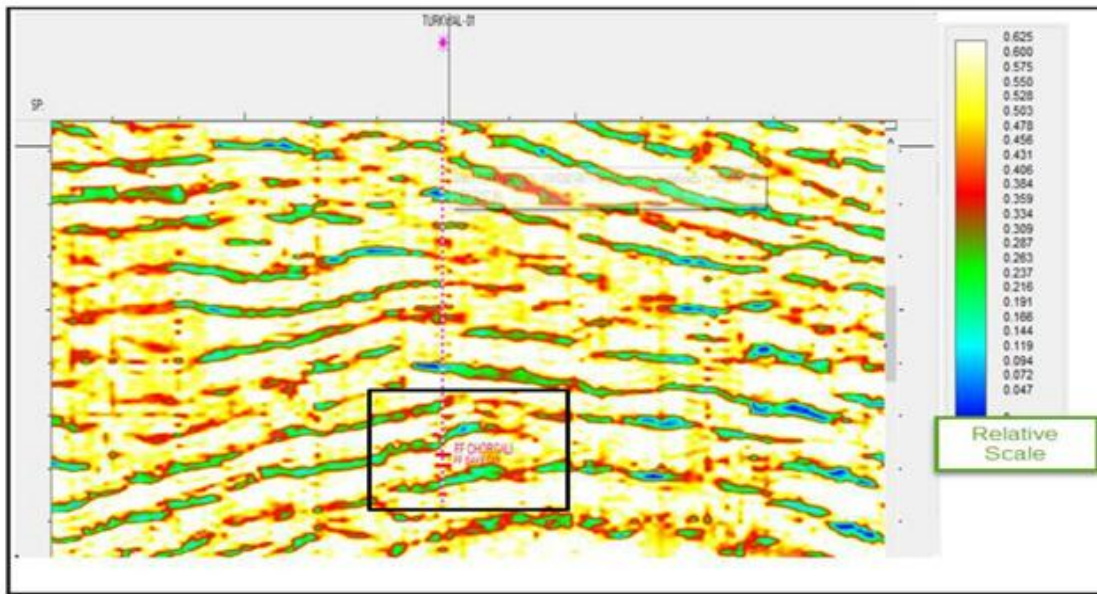


**Figure (5.11): Inverted seismic section.**

## 5.7 Interpretation of inverted section:

After convolution of seismogram with mean spectrum an inverted seismic section is generated as shown in above figures (5.12). The inverted section can be interpreted by using color bar. The white to yellow color shows high values of acoustic impedance and blue to green color shows low impedance.

The hydrocarbons accumulation is associated with low acoustic impedance. The given inverted section is shown with T-D chart and it shows Formations as well. The Formation circled in figure (5.12) is Chorgali and it yields a response of low acoustic impedance it is related to presence of hydrocarbon accumulation it is also confirmed from Petrophysical results.

The Chorgali is interpreted as most producing reservoir in Fimkessar area. Because results obtained from seismic inversion shows low values of impedance and structure formed is anticline both conditions give indication for presence of hydrocarbons. The zoomed view of figure (5.13) also confirms our results.

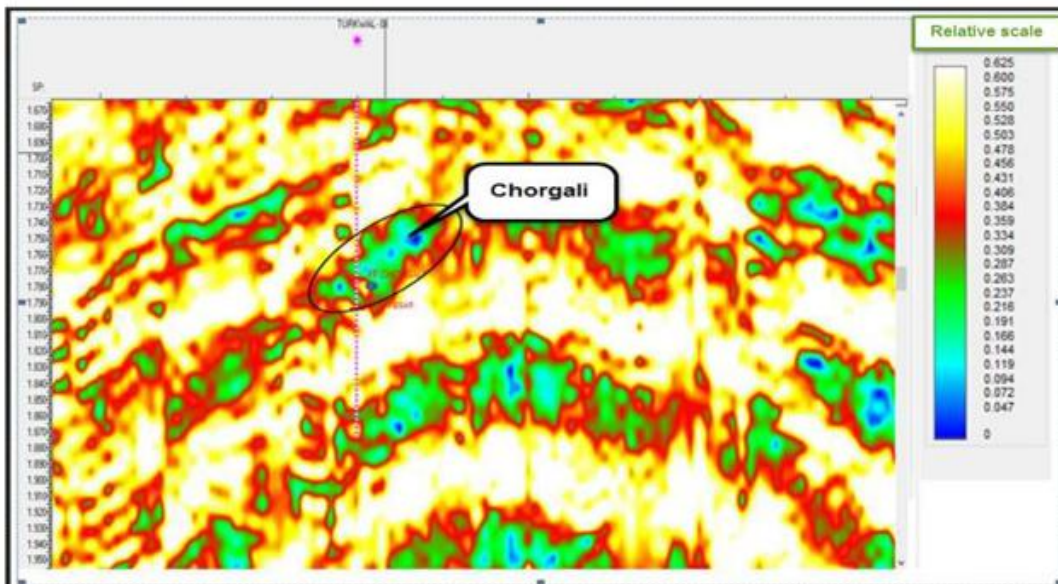


Figure (5.12): Zoomed view of inverted section.

## 5.8 Confirmation of lead-02:

The lead-02 is marked on three ways dip structure known as snaked head structure. This lead represents time (1.843s) at Chorgali Formation. This lead is confirmed by using results of seismic inversion we observed at lead-01 as reference. The snaked head structure marked at



(1.843s) and lies exactly below 555 shot point as highlighted in a picture by black rectangle in figure (5.13).

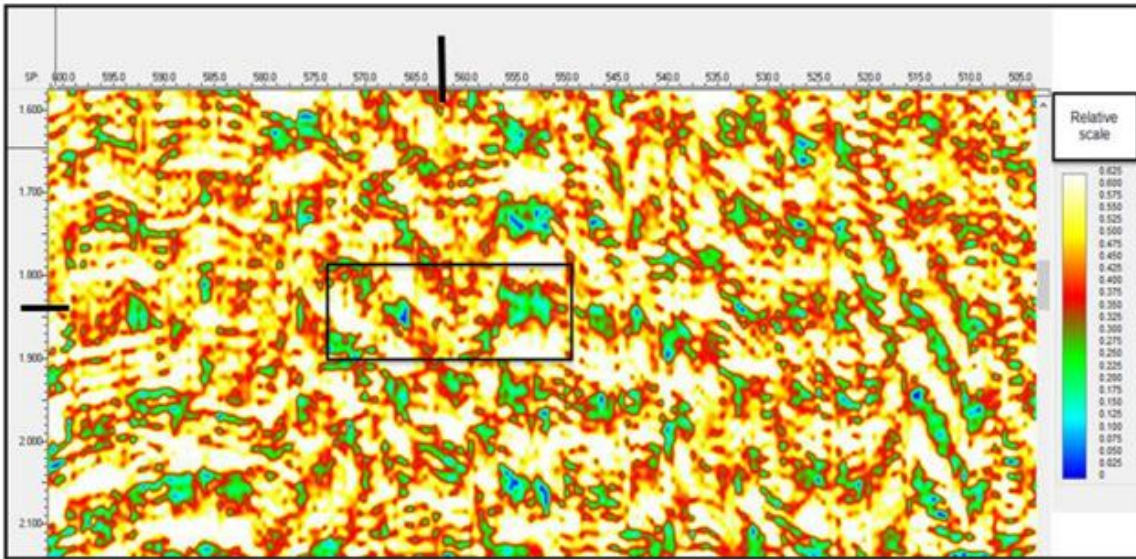


**Figure (5.13): Highlights snaked head structure at inverted section.**

If we zoom the highlighted area then we can interpret this area yields low acoustic impedance values. As Chorgali is most producing reservoir rock in upper Indus basin also found to be most producing rock in Fimkessar area.

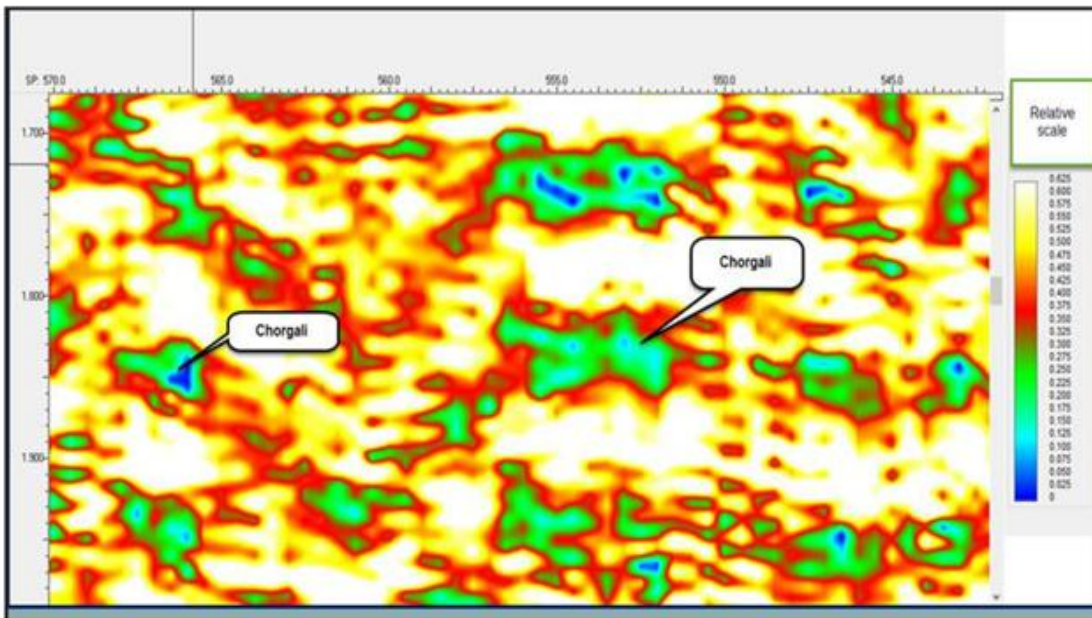


**Figure (5.14): Zoomed view of snaked head structure i.e. lead-02.**

**Conclusion:**

- Subsurface seismic data interpretation of Fimkessar area indicates an anticlinal structure and associated faulting on limbs of the anticline and snaked head structures.
- The clays and Shales of the Murree Formation also provide efficient vertical and lateral seal to Eocene reservoirs wherever it is in contact.
- Snaked head and anticlinal structures are also confirmed by attribute analysis.
- Seismic inversion and Petrophysical interpretation of Chorgali Formation indicates that it is most productive reservoir rock in study area.
- The both lead-01 and lead-02 are marked on anticlinal and snaked head structure respectively. The well is already drilled at lead-01 that is used as a reference to confirm Lead-02. The lead-02 is confirmed by using seismic inversion results.

## References:

- Asquith, G.B., and Gibson, C.R., 2004. Basic well log analysis, 2<sup>nd</sup> edition.
- Badley, M.E, 1985. Practical seismic interpretation.
- Brown, A. R. (1996). Seismic attributes and their classification. The leading edge, 15(10), 1090-1090.
- Chew, W. C., Nie, Z., Liu, Q. H., & Anderson, B. (1991). An efficient solution for the response of electrical well logging tools in a complex environment. IEEE Transactions on Geoscience and Remote Sensing, 29(2), 308-313.
- Clark, B., Bonner, S. D., Jundt, J., & Luling, M. (1993). U.S. Patent No. 5,235,285. Washington, DC: U.S. Patent and Trademark Office.
- Coffeen, J.A., 1986. Seismic exploration fundamentals, Penn Well Publishing Company, Tulsa, Oklahoma
- Dix, C. H., 1955, Seismic Velocities for Surface Measurements, Geophysics, Vol 20, pp. 68-86.
- Gardner, G.H.F., Gardner, L.W., and Gregory, A.R., 1974, Formation velocity and density – the diagnostic basics for stratigraphic traps: Geophysics, 39, 770-780.
- Gluck, S., Deschizeaux, B., Mignot, A., Pinson, C., & Huguet, F. (2000). Time-lapse impedance inversion of post-stack seismic data. In SEG Technical Program Expanded Abstracts 2000 (pp. 1509-1512). Society of Exploration Geophysicists.
- Hearst, J. R., & Nelson, P. H. (1985). Well logging for physical properties.
- Hürlimann, M. D. (2012). Well logging. eMagRes.
- Kadri, I.B, 1995, Petroleum Geology of Pakistan, PPL Pakistan.640
- Kazmi A.H and Jan M.Q, 1997, P 186-188
- McQuillin, R., Bacon, M., & Barclay, W. (1984). An introduction to seismic interpretation-Reflection seismics in petroleum exploration.
- McQuillin, R., Bacon, M., and Barcaly, W., 1984 An introduction to seismic interpretation, Graham & Trotman Limited Sterling House, 66 Wilton Road London SW1V 1DE
- Pendrel, J., "Seismic Inversion—A Critical Tool in Reservoir Characterization", Scandinavian Oil-Gas Magazine, No. 5/6, 2006, p. 19-22
- Pendrel, J., "Seismic Inversion—The Best Tool for Reservoir Characterization", CSEG Recorder
- Plummer, CC., McGerry, D., and Carlson, D.H., 2005. Physical Geology: 10<sup>th</sup> edition.
- Russell, B. H. (1988). Introduction to seismic inversion methods. Society of Exploration Geophysicists.



- Russell, B., & Hampson, D. (1991). Comparison of poststack seismic inversion methods. In SEG Technical Program Expanded Abstracts 1991 (pp. 876-878). Society of Exploration Geophysicists.
- Yilmaz.2001, Seismic Data Analysis and Processing, Inversion and Analysis of Seismic Data, Society of Exploration Geophysics, Tulsa